CHARACTERIZATION OF WHEY PROTEIN ISOLATE AND XYLAN COMPOSITE FILMS WITH AND WITHOUT TRANSGLUTAMINASE

By

Karl Josef Seiwert

A THESIS

Submitted to
Michigan State University
in partial fulfillment of the requirements
for the degree of

Food Science—Master of Science

2020

ABSTRACT

CHARACTERIZATION OF WHEY PROTEIN ISOLATE AND XYLAN COMPOSITE FILMS WITH AND WITHOUT TRANSGLUTAMINASE

By

Karl Josef Seiwert

When used as packaging materials, composite edible films exhibit improved properties over those made from individual components alone. This study investigated whey protein isolate films containing 10 – 40 g xylan / 100 g whey protein isolate (WPI). Transglutaminase (TG) was used as a cross-linking agent in WPI-only and 40 g xylan / 100 g WPI films. Food packaging properties investigated were water vapor permeability (WVP), oxygen permeability (OP), tensile stress, and % elongation at break. Thermal properties were studied using differential scanning calorimetry and thermogravimetric analysis. Crystallinity and microstructure were assessed using X-ray diffraction (XRD) and scanning electron microscopy, respectively.

Films containing 40 g xylan / 100 g WPI that were also treated with TG showed the greatest improvement over control films in properties important to food packaging. WVP decreased from 6.41 to 3.89 g mm/m² day kPa (p \leq 0.05), OP decreased from 21.85 to 7.32 cc μ m/m² day kPa (p \leq 0.05), and tensile stress increased from 6.73 MPa to 15.96 MPa (p \leq 0.05). The % elongation at break decreased significantly from 12.5% in WPI-only films to 5.8 – 1.4 % in all xylan and TG treated films (p \leq 0.05). The temperature of melting increased from 121°C in control films to a maximum of 166°C in the 20 g xylan / 100 g WPI films, indicating increased intermolecular strength. Film microstructure showed organization of xylan within films. Crystallinity was identified with increasing xylan content through XRD analysis, indicating increased polymer packing.

Dedicated to my parents, Andrew and Anna Seiwert, for all their love, support, patience, and raising me to be the person I am today

ACKNOWLEDGEMENTS

I would like to give a special thanks to Dr. Zeynep Ustunol, my advisor, for her incredible support during this master's program. Her guidance enabled me to truly feel like this research was my own, and her understanding allowed me to pursue my non-research interests in product development and sensory evaluation. This helped to make returning to school one of the most rewarding decisions I have ever made.

I would also like to thank my committee members Dr. Donatien Pascal Kamdem and Dr. Elliot Ryser, as well as Gary Smith for their guidance in the graduate program and in my research, and Dr. Didem Sutay Kocabaş for helping me get the research started and giving me advice for the road ahead. A big thanks to Michigan State University's School of Packaging, and especially Aaron Walworth, whose instrumentation support and instruction was a fundamental part of my research. Another thanks to the MSU Dairy Foods Complex and its staff for their support in my education. I would like to acknowledge Grande Custom Ingredients Group and Ajinomoto Health & Nutrition North America, Inc. for their donations of whey protein isolate and transglutaminase, respectively. Another acknowledgement to the USDA-FAS for funding this research.

I would like to thank the Food Science and Human Nutrition department's staff and faculty for their continued support, guidance, and knowledge. Lastly, a special thanks to the graduate students and their friendships during my studies here at Michigan State University.

TABLE OF CONTENTS

LIST OF TABLES	vii
LIST OF FIGURES	ix
KEY TO ABBREVIATIONS	xi
1. INTRODUCTION	1
2. LITERATURE REVIEW	4
2.1. Edible Protein Films	4
2.1.1. Film Components	5
2.1.2. Film Formation Process	5
2.2. Composite Film Individual Component Properties	6
2.2.1. Whey Protein	
2.2.2. Hemicellulose	
2.2.2.1. Xylan	11
2.2.2.2. Xylan in Films	
2.2.3. Plasticizer	
2.2.4. Cross-linking Agent	
2.3. Food Packaging Properties	14
2.3.1. Barrier Properties	
2.3.1.1. Water Vapor Permeability	
2.3.1.2. Oxygen Permeability	17
2.3.2. Mechanical Strength	
2.3.2.1. Tensile Stress & % Elongation at Break	
2.4. Structural Characterization	
2.4.1. X-Ray Diffraction	19
2.4.2. Scanning Electron Microscopy	20
2.5. Thermal Properties	21
2.5.1. Differential Scanning Calorimetry	
2.5.2. Thermogravimetric Analysis	21
3. MATERIALS AND METHODS	23
3.1. Materials	23
3.2. Film Preparation	
3.3. Physical Properties	
3.3.1. Film Thickness	
3.3.2. Moisture Content (MC)	
3.3.3. Density	
3.3.4. Color	
3.4. Properties Impacting Food Application	
3.4.1. Mechanical Properties	
3.4.2. Water Vapor Permeability	

3.4.3. Oxygen Permeability	30
3.5. Film Characterization	30
3.5.1. Ultra-violet Light Absorbance	30
3.5.2. X-Ray Diffraction	
3.5.3. Microstructure	31
3.5.4. Thermogravimetric Analysis	31
3.5.5. Differential Scanning Calorimetry	
3.6. Statistical Analysis	
4. RESULTS & DISCUSSION	33
4.1 Film Formulation	
4.2 Film Description	
4.3 Color	
4.4. Properties Impacting Food Application	38
4.4.1. Water Vapor Permeability	
4.4.2. Oxygen Permeability	40
4.4.3. Mechanical Properties	
4.5. Film Characterization	
4.5.1. Crystallinity	43
4.5.2. Microstructure	
4.5.3. Differential Scanning Calorimetry	
4.5.4. Thermogravimetric Analysis	50
5. CONCLUSIONS	52
6. RECOMMENDATIONS	53
APPENDICES	54
APPENDIX A: Material Specs	55
APPENDIX B: Preliminary Experiments	
REFERENCES	68

LIST OF TABLES

Table 1: Percentage of amino acids in selected whey protein fractions (Morr & Ha, 1993)
Table 2: The effect of increased crystallinity on selected polymer properties (Selke & Culter, 2016)
Table 3: Film treatment formulations of whey protein isolate (WPI) with increasing levels of xylan (Xy) and crosslinking by transglutaminase (TG)
Table 4: Edible whey protein isolate (WPI) film component masses required to prepare 150mL of film forming solution. WPI films were treated with xylan (Xy) and transglutaminase (TG)
Table 5: Thickness, % moisture content, and density of whey protein isolate (WPI) films prepared with xylan (Xy) at 10 to 40 g Xy/100 g WPI and transglutaminase (TG)
Table 6: Color changes in whey protein isolate (WPI) films prepared with xylan (Xy) from 10 to 40 g Xy/100 g WPI and transglutaminase (TG)
Table 7: Mechanical and barrier properties (23°C, 50% RH) of whey protein isolate (WPI) edible films with xylan (Xy) and transglutaminase (TG)
Table 8: DSC analysis from melting point curves of whey protein isolate (WPI) films prepared with xylan (Xy) and transglutaminase (TG)
Table 9: TGA analysis of whey protein isolate (WPI) films prepared with increasing xylan (Xy) content and transglutaminase (TG)
Table 10: Xylan compositional analysis from Megazyme's specification sheet
Table 11: Whey protein isolate compositional specifications from Grande Ingredients Group 5:
Table 12: Typical amino acid profile of whey protein isolate provided by Grande Ingredients Group (grams amino acid per 100 grams protein)
Table 13: Preliminary experiment (1 of 5) treatment formulations for whey protein isolate (WPI) crosslinked with transglutaminase (TG)
Table 14: Preliminary experiment (2 of 5) treatment formulations for whey protein isolate (WPI) and xylan composite films crosslinked with transglutaminase (TG)
Table 15: Preliminary experiment (3 of 5) treatment formulations for whey protein isolate (WPI) and xylan composite films crosslinked with transglutaminase (TG)

Γable 16: Preliminary experiment (4 of 5) treatment formulations for whey protein isolate (WPI)
and xylan composite films crosslinked with transglutaminase (TG)
Table 17: Preliminary experiment (5 of 5) treatment formulations for whey protein isolate (WPI)
and xylan composite films crosslinked with transglutaminase (TG)

LIST OF FIGURES

Figure 1: Arrangement of lignocellulosic biomass matrix and its three component layers 10
Figure 2: Chemical structure of aldopentose D-xylose in chair conformation, Fisher projection, and Haworth projection (Peña et al., 2013)
Figure 3: Xylan polymer chain containing a methylated glucuronic acid side chain (Naidu et al., 2018)
Figure 4: The crosslinking reaction catalyzed by transglutaminase between glutamine (Gln) and lysine (Lys) residues (Kieliszek & Misiewicz, 2014)
Figure 5: Net flux of permeants through a package wall
Figure 6: Scheme for preparation of whey protein isolate (WPI) based films
Figure 7: Yellowing of whey protein isolate (WPI) films prepared with xylan (Xy) from 10 to 40 g Xy/100 g WPI and transglutaminase (TG)
Figure 8: Absorbance of whey protein isolate (WPI) edible films prepared with xylan (Xy) and transglutaminase (TG) at 200 to 300 nm
Figure 9: Water vapor permeability (WVP) coefficients for whey protein isolate (WPI) edible films as a function of xylan content and transglutaminase (TG)) (23°C, 50% RH)
Figure 10: Oxygen permeability (OP) coefficients for whey protein isolate (WPI) edible films as a function of xylan content and transglutaminase (TG) (23°C, 50% RH) 4
Figure 11: Tensile stress of whey protein isolate (WPI) edible films as a function of xylan content and transglutaminase (TG) treatment)
Figure 12: Percent Elongation at break of whey protein isolate (WPI) edible films as a function of xylan content and transglutaminase (TG)
Figure 13: XRD analysis of whey protein isolate (WPI) films with xylan (Xy) and transglutaminase (TG)
Figure 14: Surface microstructure of whey protein isolate (WPI) films prepared with xylan (Xy) and transglutaminase (TG). Images captured through SEM at 500x magnification
Figure 15: Microstructure of fractured film edge of whey protein isolate (WPI) films prepared with xylan (Xy) and transglutaminase (TG). Images captured through SEM at 500x magnification.

Figure 16: DS	SC profiles of whey protein isolate (WPI) films prepared with 40 g xylan / 100 g WPI (WPI-Xy40) and transglutaminase (TG)	49
Figure 17: TO	GA profiles of whey protein isolate (WPI) films treated with 40 g xylan / 100g WI (WPI-Xy40) and transglutaminase (TG)	
Figure 18: Pre	eliminary experiment results (1 of 5) for whey protein isolate (WPI) standalone films crosslinked with transglutaminase (TG)	.58
Figure 19: Pre	eliminary experiment results (2 of 5) for whey protein isolate (WPI) and xylan standalone films crosslinked with transglutaminase (TG)	.60
Figure 20: Pre	eliminary experiment results (3 of 5) for whey protein isolate (WPI) and xylan standalone films crosslinked with transglutaminase (TG)	.62
Figure 21: Pre	eliminary experiment results (4 of 5) for whey protein isolate (WPI) and xylan standalone films crosslinked with transglutaminase (TG)	.64
Figure 22: Pre	eliminary experiment results (5 of 5) for whey protein isolate (WPI) and xylan standalone films crosslinked with transglutaminase (TG)	.66
Figure 23: Cr	ystallization of the plasticizer sorbitol in whey protein isolate films after conditioning for 7 days	67

KEY TO ABBREVIATIONS

BSA Bovine Serum Albumen

DSC Differential Scanning Calorimetry

%E Percent Elongation at Break

FFS Film Forming Solution

HC Hemicellulose

Ig Immunoglobulin

LA α-lactalbumin

LG β-lactoglobulin

MC Moisture Content

OP Oxygen Permeability

PS Polysaccharide

RH Relative Humidity

SCCM Standard Cubic Centimeters per Minute

SEM Scanning Electron Microscopy

TG Transglutaminase

TGA Thermogravimetric Analysis

TS Tensile Stress

WPC Whey Protein Concentrate

WPI Whey Protein Isolate

WVP Water Vapor Permeability

WVTR Water Vapor Transmission Rate

XRD X-ray Diffraction

Xy Xylan

YI Yellowness Index

1. INTRODUCTION

An increasing amount of packaging over the years has been produced from non-biodegradable, petroleum-based materials, with over 14 million tons of plastic containers and packaging produced by the United States in 2017 alone (US EPA, 2017). As concern for the environment grows, biodegradable polymers produced from proteins, polysaccharides (PS), and lipids are becoming increasingly attractive solutions to reducing packaging waste. One avenue where these biopolymers have been utilized is in edible films for primary food packaging that directly contacts the food. Such packaging materials must improve quality, food safety, and shelf life without negatively impacting the product. This is accomplished through providing a barrier to gases, moisture, and organic vapors, as well as mechanical strength to prevent physical harm. Biopolymers also have the added benefit of incorporated functionality. They can add flavors, colors, antioxidants, nutritive value, and antimicrobial capabilities to packaging (Galus & Kadzińska, 2015).

Whey, a waste byproduct of cheese production, can be processed through fractionation to produce whey protein isolate (WPI), a value-added product containing at least 90% protein (Yadav et al., 2015). These globular proteins have very good film-forming capability, and have been widely utilized in the formulations of edible films and coatings. Recent applications of WPI packaging have improved the quality of cooked meats, fresh cheeses, and seafood (Akcan et al., 2017; Gurdian et al., 2017; Shokri et al., 2015). The utility of WPI films stems from their moderate mechanical strength and excellent barrier properties to nonpolar gases and aroma compounds at low relative humidity (RH). However, their hygroscopic nature makes them poor barriers to moisture (Hassan et al., 2018). To improve film quality, the incorporation of other

macromolecules can be used to form composite films that contain new properties, with components working together synergistically. With WPI films, this has been accomplished through the addition of lipids to improve water vapor permeability (WVP), or PS to improve mechanical strength (Galus & Kadzińska, 2016; Jiang et al., 2016).

Composite films combining WPI with PS have been produced using cellulose nanocrystals, where both improved mechanical strength and decreased WVP were observed (Qazanfarzadeh & Kadivar, 2016; Sukyai et al., 2018). While the extracted cellulose used in these studies contained some hemicellulose (HC), there was no research available on effect of the purified HC xylan combined with WPI. HC, a renewable resource obtained from plant biomass, is the second most abundant biopolymer in nature after cellulose (Ebringerová & Heinze, 2000). It can be obtained from post-harvest waste material, possibly providing added value to the life cycle of crops (Naidu et al., 2018). Xylan is the most common HC and has been shown to have film forming abilities under the right conditions (Goksu et al., 2007; Zhang & Whistler, 2004). One study incorporating xylan into wheat gluten protein yielded films with lower WVP (Kayserilioğlu et al., 2003).

In addition to combining biomolecules to form composite films, cross-linking agents can also be used to improve some film properties by covalently bonding previously unassociated film components. Transglutaminase (TG) is a cross-linking enzyme that has been used in WPI films to decrease WVP and increase mechanical strength (Jiang et al., 2016). By incorporating xylan into WPI films and cross-linking with TG, a composite film could be created with improved barrier properties and mechanical strength, possibly opening new applications and improved food packaging quality.

The main objective of this study was to test the hypothesis that a WPI edible film with incorporated xylan will have greater mechanical and barrier characteristics than a film without xylan. In this work we propose to incrementally increase the xylan added in the WPI film in an attempt to find the optimal quantity needed to maximize WPI film properties. The effect of TG was tested on the best performing xylan treatment.

After the successful development of standalone films, the objectives of this research were:

- 1. To compare the mechanical strength of films with and without xylan, expressed as tensile stress and % elongation at break.
- 2. To determine the WVP and oxygen permeability (OP) of films with and without xylan.
- 3. To quantify the effect of xylan addition with respect to film color using a yellowness index.
- 4. To determine thermal properties of films with and without xylan
- 5. To evaluate the films' microstructures to determine if structural organization relates to physical characterization measurements.

2. LITERATURE REVIEW

2.1. Edible Protein Films

Edible protein films have been produced from soy protein, corn zein, wheat gluten, and whey protein (Hassan et al., 2018). It is reported that a globular protein's ability to form films is directly related to the bonding properties of the amino acid residues on the protein. These bonds make up the secondary structure of a protein, and include hydrogen bonding, hydrophobic interactions, salt bridges, disulfide linkages, and van der Waals forces. The secondary structure informs a protein's native state (tertiary structure). To make a film from protein, its original secondary interactions are disrupted to some degree while in solution, and the solution is cast (Jiang et al., 2019) or extruded (Janjarasskul et al., 2014) with new interactions that produce a film. The breakdown and formation of new disulfide bonds between cysteine residues is often cited as a major component of film formation in proteins (Ramos et al., 2012).

The properties of the amino acid residues' intermolecular forces are what make protein films a promising area of research. They allow for the incorporation of additional biomolecules in composite films, or additives in active packaging. The application of edible films focuses on food preservation and extending shelf life by prolonging the time before a food decreases in quality. This is accomplished by reducing oxidation, moisture absorption, or microbiological degradation of the food. One recent promising application has been the development of edible films made from the milk protein casein, a globular protein. A team from the USDA's Agricultural Research Service led by Peggy Tomasula improved oxgyen barrier properties with the incorporation of pectin or treatment with alkali compounds. Soluble films were used to create soup and instant coffee packets, and less soluble, more moisture resistant protein coatings were applied to cereals to keep the product crunchy longer in milk (O'Brien, 2018).

2.1.1. Film Components

Edible protein films consist of at least two simple components: a globular protein and a plasticizer. Proteins are hydrocolloids – high molecular weight compounds that can form a gel in water. These biopolymers provide the strength and bulk for the film. However, alone they produce brittle, inflexible films that cannot provide the functionality required for food packaging. The addition of a low molecular weight compound such as glycerol or sorbitol is required to plasticize the film. The addition of plasticizer will increase the WVP and improve the flexibility of the film (McHugh & Krochta, 1994). These compounds are the base components required to produce films of moderate strength with excellent oxygen, and poor moisture barrier properties (Hassan et al., 2018).

Most research has focused on improving film qualities important to food packaging: barrier properties and mechanical strength. In addition to forming composite films with PS, cross-linking agents can improve protein films. Cross-linking agents allow for the formation of extra covalent bonds in the film, adding to its strength and barrier properties. The enzyme TG and compound genipin are two successful protein cross-linking agents that have been used in edible films (Jiang et al., 2016; Lin et al., 2020).

2.1.2. Film Formation Process

Protein films are produced by dissolving the protein in a solvent, commonly water or ethanol, to make the film forming solution (FFS). To optimize the protein's film forming ability, the FFS may need further alteration which can be accomplished through various means: temperature treatment, pH adjustment, sonication, and physical disruption through homogenization (Galus & Kadzińska, 2016; Jiang et al., 2016). The main goal at this stage is the alteration and disruption of the intramolecular forces so new, intermolecular forces can develop

and make a film. The plasticizer is added to the FFS, along with any experimental additives (additional hydrocolloids, antimicrobials, etc.).

To produce the actual film, the FFS is cast onto a flat surface and dried. Wet casting is most common, however such films can lack uniformity depending on the casting surface and the process is generally inefficient for industrial applications. Large scale extrusion of dry film ingredients such as proteins is possible, but not all materials lend themselves to the extrusion process and the cost may be prohibitive (Chevalier et al., 2018). Film conditioning in a controlled chamber of specific RH and temperature is the final step before characterization according to standard testing methods.

2.2. Composite Film Individual Component Properties

All edible film characteristics – which define performance – are dependent on the film components and their chemistry. WPI's amino acid makeup defines the molecular forces that allow the film to form. The addition of glycerol as a plasticizer and transglutaminase as a cross-linking agent is common. The HC xylan is a potential hydrocolloid for use in composite films. It is important to understand the chemistry of each film component when developing films having specific characteristics.

2.2.1. Whey Protein

Milk proteins are characterized in one of two groups: caseins and whey proteins. Caseins can be broken down into four subgroups that together form a micellular structure that precipitates from milk at pH of 4.6. Whey proteins are the remaining proteins that are still soluble at pH of 4.6 (Farrell et al., 2004). The largest contributing whey proteins are β-lactoglobulin (LG) (60%), α-lactalbumin (LA) (20%), bovine serum albumin (BSA) (3%), and

Immunoglobulins (Ig) (10%) (Edwards & Jameson, 2014). The component amino acid residue's bonding activity is integral to the protein's reactivity. Amino acid compositions for select whey protein fractions are detailed in Table 1.

LG is a globular protein consisting of 162 amino acid residues with a molecular weight of 18.3 kDa (Morr & Ha, 1993). It contains two disulfide bonds, one sulfhydryl group, and various hydrophobic regions. In its native form these intramolecular bonds are turned inward, preventing aggregation. However, at temperatures above 60°C LG will partially denature, making these regions available for intermolecular bonding. At that temperature the protein will begin to gel or form aggregates – a process directly related to time and temperature (Nicolai et al., 2011). Ideally, reactive LG is only partially denatured to form new protein-protein interactions, while still retaining some of its native form to avoid complete aggregation.

LA has a molecular weight of 14 kDa and a total of 123 amino acid residues. It contains 6.5% cystine residues which contribute to its four disulfide bonds (Heine et al., 1991; Morr & Ha, 1993). Calcium acts as a stabilizing factor in the protein, and its presence influences the denaturation temperature of the protein. With adequate calcium present, denaturation occurs at 65°C (Griko & Remeta, 1999).

BSA, a blood serum protein, consists of 582 amino acids and has a molecular weight of 69 kDa (Morr & Ha, 1993). This larger protein has a greater number of cysteine residues, contributing to its 17 disulfide bonds (Farrell et al., 2004). BSA will form aggregates at elevated temperatures and neutral pH, with ordered structure in the form of β-sheets and febrils (Holm et al., 2007). These changes have been observed at 70°C, with most secondary structure changes occurring in 60 minutes (Militello et al., 2003).

Table 1: Percentage of amino acids in selected whey protein fractions (Morr & Ha, 1993) Note: $LG = \beta$ -lactoglobulin; $LA = \alpha$ -lactalbumin; BSA = bovine serum albumin

_	Whey Protein Fraction				
Amino Acid Residue	% of LG	% of LA	% of BSA		
Asp	6.2	7.3	6.7		
Asn	3.1	9.8	2.1		
Thr	4.9	5.7	5.8		
Ser	4.3	5.7	4.8		
Glu	9.9	6.5	10.1		
Gln	5.6	4.1	3.3		
Pro	4.9	1.6	4.8		
Gly	2.5	4.9	2.7		
Ala	9.3	2.4	7.9		
Cys	3.1	6.5	6.0		
Val	5.6	4.9	6.2		
Met	2.5	0.8	0.7		
Ile	6.2	6.5	2.4		
Leu	13.6	10.6	10.5		
Tyr	2.5	3.3	3.3		
Phe	2.5 3.3		4.6		
Lys	9.3	9.8	10.1		
His	1.2	2.4 2.9			
Trp	1.2	3.3	0.3		
Arg	1.9	1.9 0.8 4.0			

Igs are glycoproteins that range in size from 15 to 1000 kDa. Igs individually have a higher denaturation temperature than LG and LA but have been found to be thermolabile in the presence of other whey proteins due to possible interaction with LG and BSA through the formation of disulfide bonds (Morr & Ha, 1993).

Concentrated whey protein as a dry ingredient comes in the form of WPI or whey protein concentrate (WPC). Both are produced through microfiltration, a process that removes residual fat, microorganisms, lactose, and some ash before drying. The two products differ in the degree of protein purification, with WPC containing 34% to 80% protein, and WPI containing greater than 90% protein (Yadav et al., 2015).

2.2.2. Hemicellulose

Lignocellulosic biomass, the material that makes up the bulk of all plant structure, is composed of cellulose, HC, and lignin. These three polymers work together to form a microfibril infrastructure that provides rigidity in woods and grasses (Figure 1) (Brandt et al., 2013). Cellulose is the most abundant component, and consists of unbranched, repeating glucose units that are intermolecularly connected with hydrogen bonds. HC, the second most abundant, cross-links with lignin around cellulose to create the strong microfibril structure. Lignin is composed of phenolic compounds that act as a 'glue' to hold the entire structure together (Naidu et al., 2018).

HC is quite variable in structure with repeating units of hexoses, pentoses, acetylated sugars, and uronic acids, around 150 to 200 units in length (Beg et al., 2001). The most common sugars are arabinose, xylose, mannose, and galactose (Figure 2). These HC polymers contain side chains of sugars and sugar acids that cross-link with the cellulose core of the microfibril. The composition of the HC core and side chains varies greatly with respect to the plant from

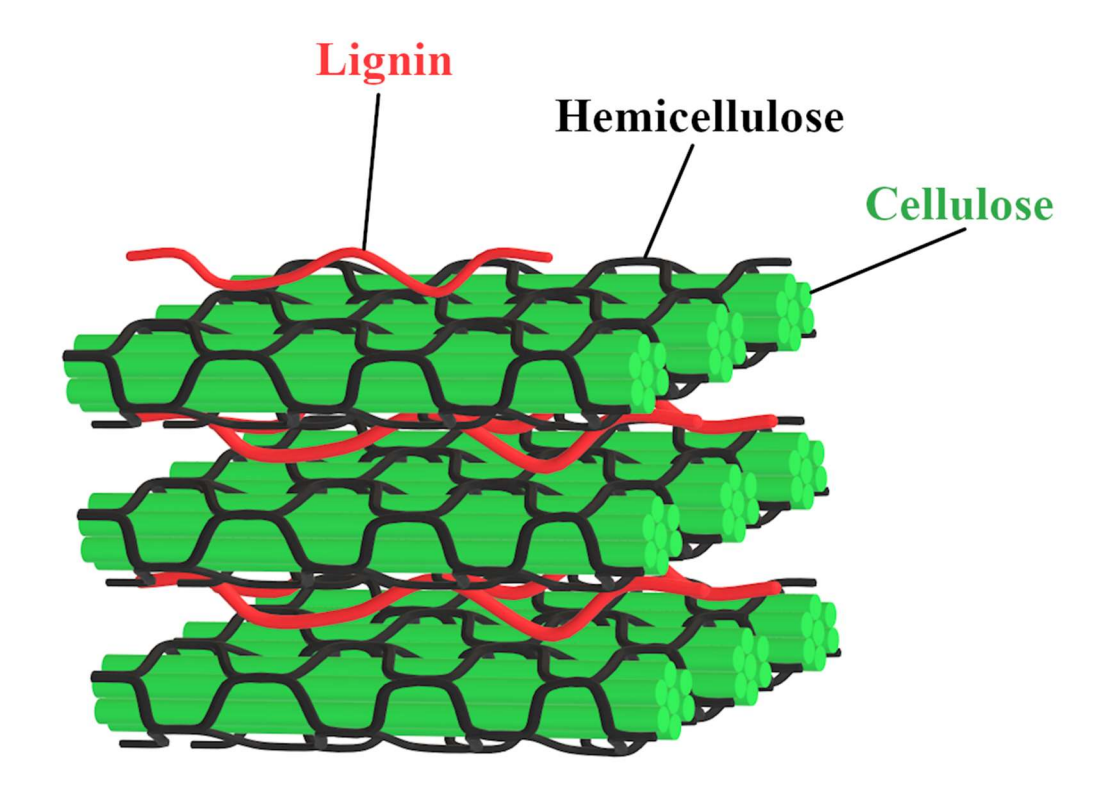


Figure 1: Arrangement of lignocellulosic biomass matrix and its three component layers

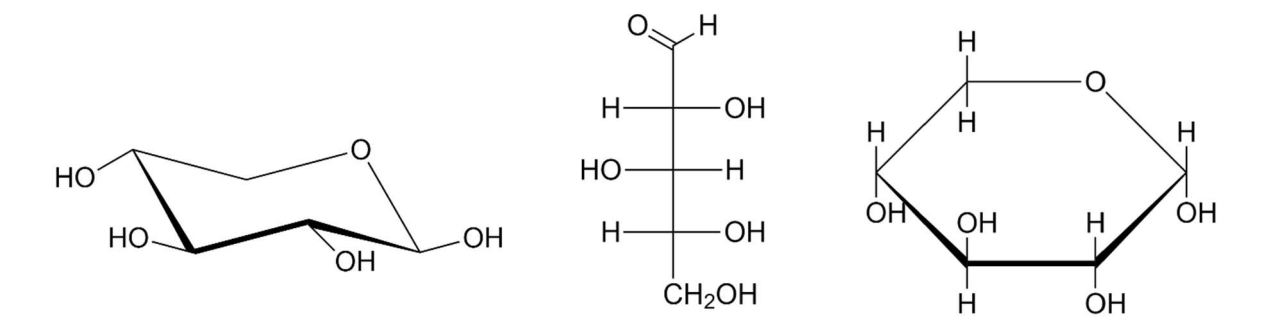


Figure 2: Chemical structure of aldopentose D-xylose in chair conformation, Fisher projection, and Haworth projection (Peña et al., 2013)

which it is derived. Xylan, the most abundant HC, can be obtained in high amounts from hardwoods, comprising up to 30% of the dry weight (Hahn-Hägerdal et al., 2001). This study focused on xylan (4-O-methyl glucuronoxylan) derived from Beech hardwood.

2.2.2.1. Xylan

The structure of xylan is variable and mainly composed of repeating xylose units connected with a β -(1,4)-linkage, substituted with 4-O-methyl glucuronosyl and acylated glucuronosyl residues (Figure 3). Arabinose may also be present in small amounts. These side chains can crosslink with cellulose via hydrogen bonding (Scheller & Ulvskov, 2010).

Because xylan is derived from a renewable resource, it is a promising avenue for future production of bio-based products. Many chemicals have been successfully manufactured from xylan, both enzymatically and with metal oxide catalysts (Naidu et al., 2018). Ethanol for fuel has been produced by fermentation with bacteria (Galbe & Zacchi, 2002). Xylitol, an artificial sweetener, is currently produced from xylan. Xylan can be hydrolyzed to xylose, which is then purified. The xylose is catalytically hydrogenated into xylitol, which is then purified and crystallized for use (Albuquerque et al., 2014). Another potential major product and area of study for xylan is its use as a packaging film.

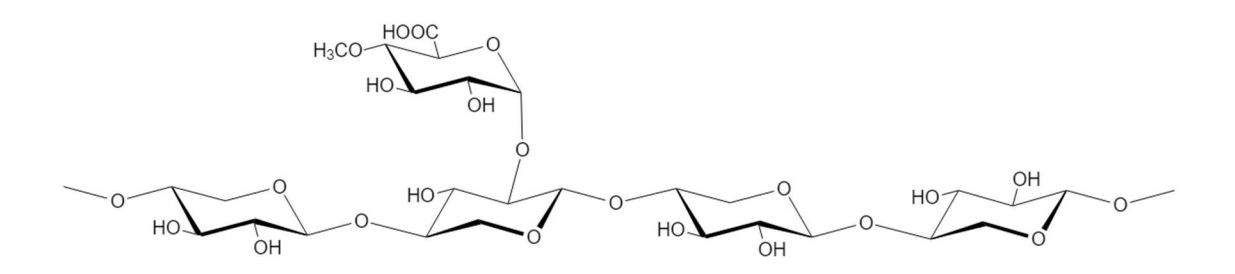


Figure 3: Xylan polymer chain containing a methylated glucuronic acid side chain (Naidu et al., 2018)

2.2.2.2. *Xylan in Films*

Xylan can form self-supporting films without the use of a plasticizer. Goksu et al. (2007) were able to produce films from xylan sourced from cotton stalks, with only about 1% lignin (w/w lignin/xylan) impurity. Mechanical properties could be improved by adding glycerol. Another study produced thin films from corn hull arabinoxylan, a xylan with high levels of arabinose. After applying the films to grapes, weight loss from moisture was reduced in the fruit by up to 41% (Zhang & Whistler, 2004). Composite films have been produced with wheat gluten containing up to at least 40% xylan (w/w xylan/wheat gluten). The processing conditions, xylan ratio, FFS pH, and xylan type all played a role in the properties of these films (Kayserilioğlu et al., 2003).

2.2.3. Plasticizer

Plasticizers are low molecular weight materials that improve the mechanical strength and flexibility of films. Sorbitol and glycerol, both sugar alcohols, are most often used in edible films. The hydroxyl groups interact with the polymer chains through hydrogen bonding, interrupting the polymer-polymer bonds. This interruption increases ductility of the film as well as its permeability to gases and moisture (Jost & Stramm, 2016). A comparison study of sorbitol and glycerol in WPI films found that sorbitol-containing films had lower OP, and films with glycerol had greater elongation. Both plasticizers produced films of comparable TS (McHugh & Krochta, 1994). In amylose-rich corn starch films, sorbitol crystallization occurred due to plasticizer migration over a period of 9 months in films with greater than 50% (w/w) sorbitol. This effect was not observed in glycerol films (Krogars et al., 2003). In composite films containing WPI and pullulan, various glycerol ratios were tested. A WPI: glycerol content of

3.6:1 produced a film that was too brittle to handle, however a ratio of 3:1 yielded good films (Gounga et al., 2010).

2.2.4. Cross-linking Agent

TG is a cross-linking enzyme that catalyzes the reaction between the γ-carboxamide group of a glutamine residue and a ε-amine group of a lysine residue to form an isopeptide bond with the release of ammonia (Figure 4) (Kieliszek & Misiewicz, 2014). The cross-linking enzyme is used to combine previously unassociated proteins, and has been used to produce films for meats, fish, baked goods, and milk products (Kieliszek & Misiewicz, 2014). Jiang et al. (2016) researched the effects of TG in composite PS/whey protein films. In their films containing WPC and carboxymethylated chitosan, TG improved functional film properties and its activity was positively identified using SDS-PAGE. This research group's WPC/nanocrystalline cellulose films with TG also showed improved mechanical properties (Jiang et al., 2019).

Figure 4: The crosslinking reaction catalyzed by transglutaminase between glutamine (Gln) and lysine (Lys) residues (Kieliszek & Misiewicz, 2014)

2.3. Food Packaging Properties

2.3.1. Barrier Properties

The metric by which a film provides a barrier to permeants like oxygen and water vapor is the permeability coefficient, P. If a film is a good barrier, it has low permeability. P is an indicator of a material's resistance to sorption and diffusion of the permeant. The three parameters are related by the following equation:

$$P = D \times S$$

where D is the diffusion coefficient and S is the solubility coefficient. D is a measure of the rate at which the permeant moves from one side of the film to the other. S describes the degree of interaction between the permeant and the film on a molecular level. Because diffusion and sorption make up permeability, any intrinsic or extrinsic factors that change S or D will affect P. These factors include the chemical composition of the film and permeant, film crystallinity, temperature, and presence of plasticizers or cross-linking agents.

Figure 5 diagrams the roles that sorption and diffusion have in the permeation process. Diffusion occurs according to Fick's law, which states that in an isotropic material, diffusion only occurs in one direction. The permeant will diffuse from an area of high concentration to low concentration in three steps. First, the permeant on the high concentration side of the film will be absorbed by the polymer. The permeant then continues to diffuse across the film, saturating the material until no more areas of low concentration remain. Finally, the permeant is desorbed from the film and moves into the low concentration side in the final step. Permeability measurements are only taken when the permeant diffuses at a constant rate. This is known as the "steady state" and is achieved when the polymer contains equal concentration of the polymer in step 2.

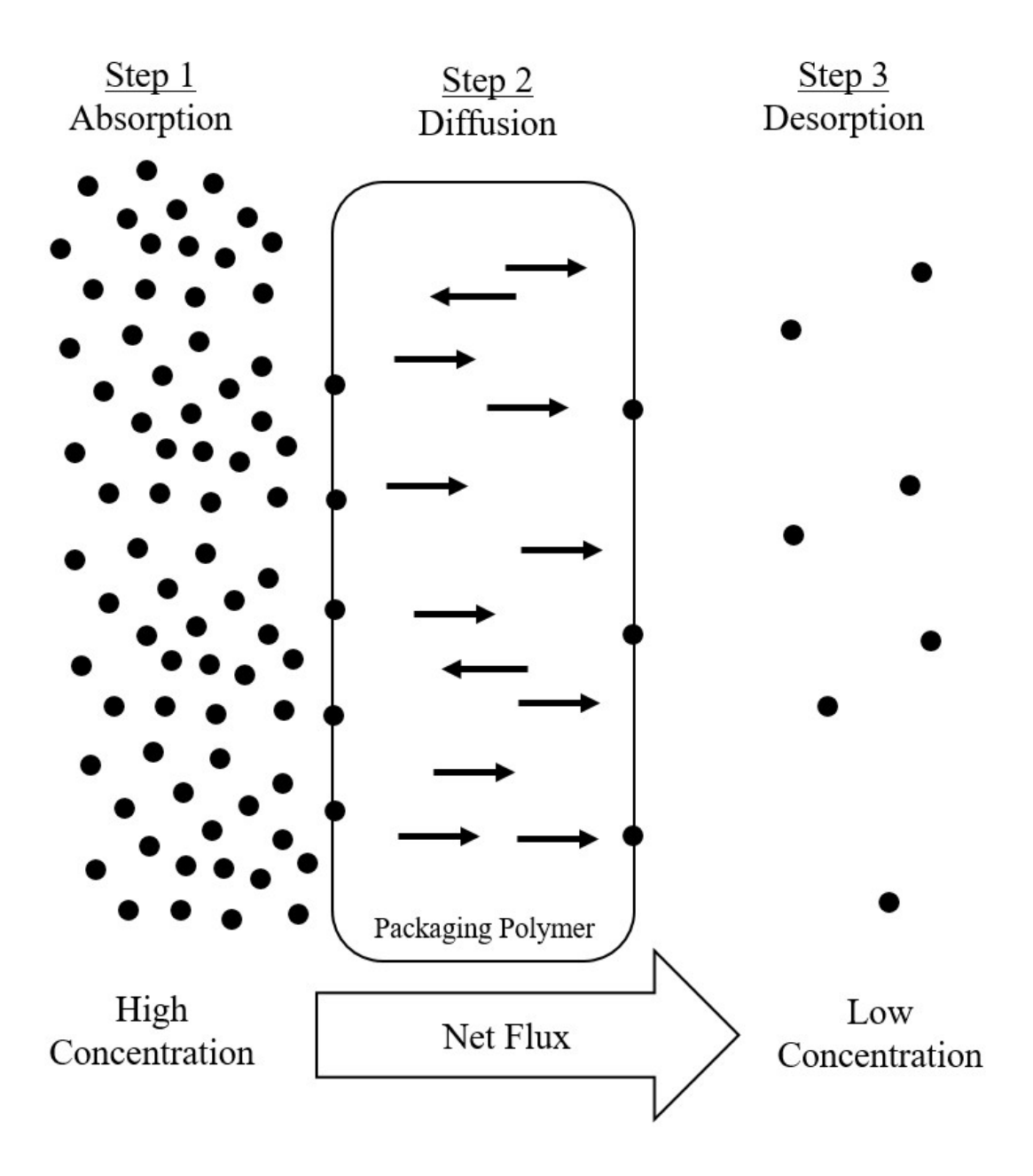


Figure 5: Net flux of permeants through a package wall

2.3.1.1. Water Vapor Permeability

The WVP of edible films can be measured by quasi-isostatic or isostatic methods. The quasi-isostatic method periodically measures the increase in water on the low concentration side of the film. WVTR is determined by plotting the quantity of water vapor as a function of time once the steady state is reached. WVP incorporates the film thickness, area, and the vapor pressure of the permeant into the WVTR:

$$WVP = \frac{WVTR \cdot l}{\Delta p \cdot A}$$

where, l is film thickness, A is film area, and Δp is partial pressure of water vapor between both sides of the film. Quasi-isostatic analysis uses gravimetric methods to determine moisture gain according to the "cup method" outlined in ASTM E96/E96M-16.

Isostatic analysis involves continually measuring permeation with no accumulation of water on the low concentration side of the film. A carrier gas, usually nitrogen, carries the water to a modulated infrared detector, where the WVTR is constantly monitored. WVP is then determined using the equation above. Because whey protein films have a high WVP, the sensitive detectors can become saturated using the isostatic approach. For this reason, the quasi-isostatic method is used most commonly. However, if the film provides an adequate barrier, the isostatic method is less labor-intensive and ASTM F1239-14 can be used.

One common method used in reducing the WVP of WPI films is the incorporation of lipids. Galus & Kadzińska (2016) incorporated walnut and almond oil at 0.5 and 1% (w/w) into WPI films plasticized with 50% (w/w) glycerol). WVP was determined gravimetrically at 100% RH and 25°C. A significant decrease in WVP was seen in films with both walnut and almond oil. The WVP of control films started at 17.3 g mm m⁻² d⁻¹ kPa⁻¹ and increased to 13.5 – 8.8 g mm m⁻² d⁻¹ kPa⁻¹ with both treatments. The incorporation of cinnamon essential oil into WPC

films had a similar effect on barrier properties. WVP decreased from 22.20 g mm m⁻² d⁻¹ kPa⁻¹ to 17.56 mm m⁻² d⁻¹ kPa⁻¹ with the addition of 1.5% (v/v) cinnamon oil (tested at 75% RH and 27°C) (Bahram et al., 2014).

The addition of polysaccharides obtained from lignocellulosic biomass have also been shown to lower WVP in composite whey protein films. WPI films containing cellulose nanocrystals from sugarcane bagasse showed reduced WVP at 50% RH and 25°C (Sukyai et al., 2018). A similar result was observed in WPI films with nanocellulose isolated from oat husk. Control films were produced using WPI and 50% glycerol conditioned at 50% RH and 35°C. The control WVP of 1.2 g mm m⁻² d⁻¹ kPa⁻¹ decreased by 14%, 34%, and 36% with the addition of the nanocellulose at 2.5, 5, and 7.5% (w/w) (Qazanfarzadeh & Kadivar, 2016).

2.3.1.2. Oxygen Permeability

OP in edible films is most often determined using isostatic methods that include coulometric detectors according to ASTM method D3985-17. Hong & Krochta (2006) evaluated the OP of plastic films coated in WPI and WPC at different temperatures and RH. OP was shown to increase with temperature by roughly two-fold every 10°C from 15°C to 40°C. This pattern followed an Arrhenius model. RH had a greater effect on OP than temperature when varied from 30% - 85% at 25°C. High moisture conditions can cause hydrophilic polymers to swell, affecting gas permeability. As a result, the lowest OP was observed at a moderate to low RH.

The incorporation of lipids into composite WPI films has shown to decrease OP. The addition of walnut and almond oil, hydrophobic compounds, improved WVP. However, they increased OP from 112.5 cc μm m⁻² d⁻¹ kPa⁻¹ to 131.5 – 157 cc μm m⁻² d⁻¹ kPa⁻¹ at the 1% (w/w)

concentration (Galus & Kadzińska, 2016). This is caused by decreasing the film's crystallinity through disruption of the protein matrix, generating channels and pores for gas movement.

Polysaccharide incorporation into WPI composite films has the advantage of not increasing OP, while still decreasing WVP. Cellulose nanocrystals from oat husks that were incorporated into WPI films had no significant effect on OP, while still decreasing WVP (Qazanfarzadeh & Kadivar, 2016). In one study on composite films of okra PS and WPI films plasticized with glycerol, the OP was shown be 2.3-fold lower in blend films than WPI films alone. This was attributed to molecular interactions, since non-polar oxygen is minimally absorbed by the polar film (Prommakool et al., 2011).

2.3.2. Mechanical Strength

Describing the mechanical strength of a packaging is commonly done by characterizing tensile stress and the elastic properties. This is accomplished by applying a physical load to the material which leads to deformation. In films, thin strips of specified length are slowly pulled at both ends by a lab instrument until the point of fracture. A common measure of this force is tensile stress (TS), which is simply the force per unit cross-sectional area. Elasticity can be quantified by % elongation (%E) at break, which describes the extent to which the film stretches before breaking. Brittle and hard films will normally have a low %E while still having improved TS (Selke & Culter, 2016).

2.3.2.1. Tensile Stress & % Elongation at Break

Whey protein films normally have moderate mechanical properties that can be affected by processing conditions as well as additives. Lipids will decrease TS due to their interruption of the film's crystallinity, whereas PS will increase TS (Galus & Kadzińska, 2016; Sukyai et al., 2018). In oat husk nanocellulose/WPI films, the addition of PS to the WPI only improved TS to

a certain point. The TS increased from 2.19 MPa to 4.25MPa for films containing up to 5% (w/w) nanocellulose, however at 7.5% (w/w) nanocellulose the TS began to decrease. The initial increase is thought to have come from a higher degree of crystallinity, however at too high a concentration, nanocellulose agglomerates may form and the effect no longer improves TS (Qazanfarzadeh & Kadivar, 2016).

TG has a strong effect on the mechanical properties of whey protein films. In a study on WPC/nanocellulose crystal films, TG significantly increased the %E for films containing up to 10% (w/w) nanocellulose in WPC. This may be the result of crosslinking between the protein and PS by TG (Jiang et al., 2019). The same research group found improved WPC film TS in chitosan composite films crosslinked with TG (Jiang et al., 2016).

2.4. Structural Characterization

2.4.1. X-Ray Diffraction

A polymer's morphology, especially its crystallinity, has a profound effect on its properties as a packaging material (Table 2). Crystallinity, defined as the regular, repeating arrangement of molecules, occurs to varying degrees within polymers. These closely packed molecules provide greater TS and form a stronger barrier to permeants (Selke & Culter, 2016). The degree of crystallinity can therefore provide insight into the molecular arrangement that determines the characteristics of the film. X-ray diffraction (XRD) is an effective way to determine the degree of crystallinity in a polymer.

In cast films, XRD will show different signature patterns for the different types of crystals, however peak intensity cannot be compared due to lack of uniformity in film thickness between samples. In an analysis of Beechwood xylan, a signature peak was identified at 20°

(Carà et al., 2013). The broadness of the peak indicates amorphous regions in the HC. Peak broadness can vary from batch to batch, given the difference in HC composition between sources. This variation can be further illustrated by the 22.5° signature of cellulose obtained from sugarcane bagasse (Sukyai et al., 2018).

Table 2: The effect of increased crystallinity on selected polymer properties (Selke & Culter, 2016)

Property	Effect
Permeability	decreases
Opacity	increases
Tensile strength	increases
Compression strength	increases
Tear resistance	decreases
Impact strength	decreases
Toughness	decreases
Ductility	decreases
Ultimate elongation	decreases
Heat sealing temperature	increases
Heat sealing range	decreases

2.4.2. Scanning Electron Microscopy

By investigating the film's microstructure through scanning electron microscopy (SEM), component organization and possible imperfections can be visually confirmed and related to film properties. In walnut and almond oil/WPI composite films, the scanning electron micrographs showed poor incorporation of the lipid into the protein matrix. This was evidenced by film surfaces with heterogeneous and rough patches. Cross-section micrographs showed phase separation between the oil (hydrophobic) and protein (hydrophilic) layers (Galus & Kadzińska, 2016). In wheat gluten/xylan composite films, the addition of xylan enlarged globular forms from pure wheat gluten films. Heterogeneity, which increased with increasing xylan levels, was

also dependent on xylan source – grass xylans showed little globular formation, whereas Birchwood xylan produced more heterogeneous films (Kayserilioğlu et al., 2003).

2.5. Thermal Properties

Thermal properties describe how a polymer behaves with changes in temperature. This information, which is critical in extruding, injecting, and heat-sealing films, can also provide insight into structural properties.

2.5.1. Differential Scanning Calorimetry

Differential scanning calorimetry (DSC) can be used to assess the thermal transitions of polymers by measuring the heat flow into a system as a function of temperature. The main transition identified in protein films is the melting temperature, T_m . This is the point at which the biopolymer shifts from a crystalline to an amorphous, melted form. The heat of fusion, ΔH_m , is the energy required to melt the crystalline form. ΔH_m will increase for more strongly bonded polymers, and decrease with more weakly bonded polymers (Selke & Culter, 2016). In one study looking at the thermal properties of composite films containing WPC, pectin, and alginate, the presence of WPC increased T_m . Increased ΔH_m values were also seen in alginate containing films, indicating a higher level of crystallinity caused by intermolecular interactions. Higher composite film T_m and ΔH_m compared to non-composite films are indicators of good miscibility of film components (Chakravartula et al., 2019).

2.5.2. Thermogravimetric Analysis

Thermogravimetric analysis (TGA) assesses the decomposition of materials by measuring the decrease in mass as a function of temperature. In TGA, the lower molecular weight compounds degrade first, followed by more firmly bound components. This

decomposition usually occurs over a range, with the temperature of maximum decomposition, T_{max} , being used to identify different film components. By evaluating the first derivative of the % weight loss with respect to temperature, the T_{max} of each degradation region can be determined as the peak maximum of the derivative. This is particularly useful in composite films, where the presence of a T_{max} distinct from the film components signifies new intermolecular interactions.

3. MATERIALS AND METHODS

3.1. Materials

WPI was donated by Grande Custom Ingredients Group (Fond du Lac, WI), and contained a minimum of 90% protein dry basis. Glycerol was purchased from Sigma-Aldrich (St. Louis, MO). Xylan, derived from Beechwood, was purchased from Megazyme (Bray, Ireland), and contained 82.3% xylose according to the manufacturer's lot analysis.

Transglutaminase (ACTIVA® TI) at a manufacturer-specified activity of 86 – 135 units/g was donated by Ajinomoto Health & Nutrition North America, Inc. (Itasca, IL). Relative percent composition profiles for xylan and WPI provided by their respective manufacturers are provided in Appendix A.

3.2. Film Preparation

Film treatment formulations are detailed in Table 3, and exact component masses required to prepare the film forming solutions are listed in Table 4. The control films were made from a WPI-only stock solution that was prepared as follows: 7.5 g WPI and 2.5 g glycerol were dissolved in 140 g deionized water to produce a stock solution of 5% (w/w) WPI at a 3:1 WPI:glycerol ratio by stirring for 30 minutes at room temperature. The solution's pH was then adjusted from 6.0 to 8.0 using approximately 4 drops of 2.0 N NaOH, and it was subsequently heated to 80 ± 5°C using a hot plate, stirring continuously. After 30 minutes of heating to allow for proper dissociation of the protein, the solution was homogenized for 1 min at 9000 rpm in a 250 mL beaker using a Polytron Model 10/35 homogenizer (Kinematica USA, Bohemia, NY) to thoroughly mix the film forming solution. The homogenized solution was poured through a double layer of cheese cloth to remove excess foam and cooled to 25°C ± 1°C in a 1000mL

Table 3: Film treatment formulations of whey protein isolate (WPI) with increasing levels of xylan (Xy) and crosslinking by transglutaminase (TG)

		g Xy /		
Treatment	Description	100 g WPI	TG (IU)	
WPI-Xy0	Control	0		
WPI-Xy10	10% xylan	10		
WPI-Xy20	20% xylan	20		
WPI-Xy30	30% xylan	30		
WPI-Xy40	40% xylan	40		
WPI-Xy0-TG	WPI + TG	0	30	
WPI-Xy40-TG	40% xylan + TG	40	30	

Table 4: Edible whey protein isolate (WPI) film component masses required to prepare 150mL of film forming solution. WPI films were treated with xylan (Xy) and transglutaminase (TG)

	WPI stock solution		Xylan stock solution			_	
Treatment	DI water (g)	WPI (g)	Glycerol (g)	DI water (g)	Xylan (g)	Glycerol (g)	TG (g)
WPI-TG	140.00	7.50	2.50				2.25
WPI	140.00	7.50	2.50				
WPI-Xy10	127.27	6.82	2.27	12.73	0.68	0.23	
WPI-Xy20	116.67	6.25	2.08	23.33	1.25	0.42	
WPI-Xy30	107.69	5.77	1.92	32.31	1.73	0.58	
WPI-Xy40	100.00	5.36	1.79	40.00	2.14	0.71	
WPI-Xy40	100.00	5.36	1.79	40.00	2.14	0.71	1.61

vacuum flask. Once cooled, the solution was vacuum degassed for 1 h, and 50 mL was cast into a 21-cm diameter Teflon[®] pan. The solution was evenly spread over the pan using a handmade spreader produced from a disposable glass long-nose Pasteur pipet. It was then placed on a flat, level, marble surface, and left to dry at room temperature for 48 h. Once dry, the film was transported to a conditioning chamber at $23 \pm 2^{\circ}$ C and $50 \pm 2^{\circ}$ RH.

For xylan-containing films, a xylan stock solution was first prepared (Table 4). Xylan and glycerol were dissolved in deionized water to produce a stock solution of 5% (w/w) xylan at a 3:1 xylan:glycerol ratio by stirring for 1 hat room temperature. The solution was added to the WPI stock solution after heating but before homogenization. WPI: xylan ratios were 1:0, 1:0.1, 1:0.2, 1:0.3, and 1:0.4 on a dry basis. TG-containing films were prepared by adding TG to the film solutions at an enzyme activity of 30 IU after cooling (Table 4). The solution was then stirred for 30 minutes at room temperature before being vacuum degassed for 1 h.

A detailed scheme for film production is shown in Figure 6. Each film formulation was replicated three times with new solutions and casts.

3.3. Physical Properties

3.3.1. Film Thickness

Film thickness was determined using a digital micrometer model 49-70 (Testing Machines Inc., Ronkonkoma, NY). The instrument had a resolution of \pm 0.003 mm and a 16 mm presser foot set to 7.3 psi. Overall film thickness was determined from the average of nine measurements from different film locations. Precaution was taken to avoid any measurements close to the film's edge, as the cast films had rough edges after peeling from the casting plate.

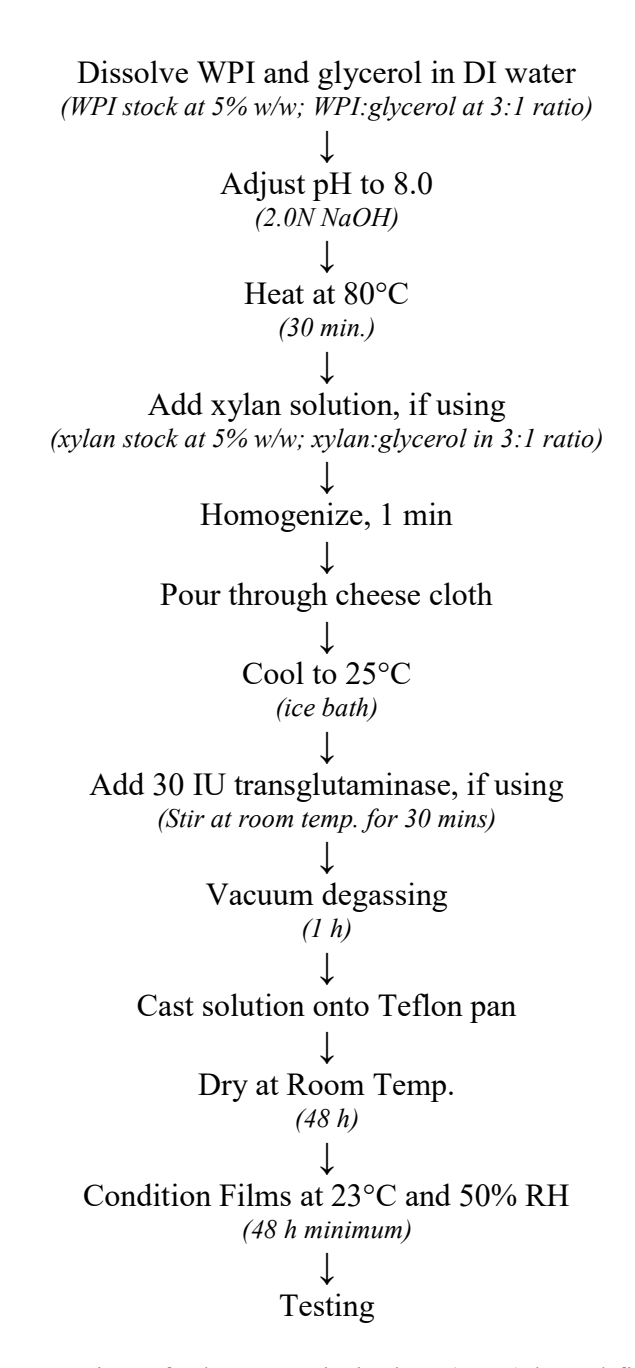


Figure 6: Scheme for preparation of whey protein isolate (WPI) based films

3.3.2. Moisture Content (MC)

MC was determined by drying the films in a vacuum oven at 100°C for 24 h (Ramos et al., 2013). Films were cut into 25.4 mm x 25.4 mm squares using a precision sample cutter and placed in aluminum pans that were weighed before and after drying. The % MC was determined on a dry basis according to the following equation:

$$\% MC = \frac{(W_i - W_D)}{W_D} \times 100\%$$

where W_i is the initial weight and W_D is the dry weight of the film.

3.3.3. Density

Density, ρ , was determined using the film's thickness, dimensions, and dry weight (Ramos et al., 2013) according to the following equation:

$$\rho = \frac{m}{A \cdot l}$$

where m is the dry mass of the film (g), A is the area of the sample (6.45 cm²), and l is the thickness. For all density calculations, the thickness used was the average thickness of the cast films and was not re-measured for each 6.45 cm² sample. Dry weight was determined by drying the films in a vacuum oven at 100°C for 24 h.

3.3.4. Color

Film color was measured using a Chroma Meter CR-400 (Konica Minolta Inc., Tokyo, Japan). A Hunter L, a, b color scale was used with illuminant 'C' and a standard observer function of 2 degrees. Before each use, the colorimeter was calibrated using a calibration plate of Yxy values Y = 88.1; x = 0.3168; and y = 0.3241.

Color was computed into total color difference, ΔE , to better highlight changes in L, a, b values using the following formula:

$$\Delta E = \sqrt{\left(L_{sample} - L_{control}\right)^{2} + \left(a_{sample} - a_{control}\right)^{2} + \left(b_{sample} - b_{control}\right)^{2}}$$

where L, a, b values were compared between each *sample* and the *control*. The yellowness index (YI) was quantified using the formula from Mehdizadeh et al.(2012):

$$YI = \frac{142.86 \cdot b}{L}$$

3.4. Properties Impacting Food Application

3.4.1. Mechanical Properties

Mechanical properties were analyzed using a modification of ASTM standard D882 – 18, "Standard Test Method for Tensile Properties of Thin Plastic Sheeting" (ASTM, 2018). A Universal Testing Machine model 5565 (Instron, Norwood, MA), calibrated annually by a trained representative from Instron, was used. This proprietary calibration process includes a full test of the instrument's data acquisition, uncertainty analysis, and checks against ISO and ASTM requirements. Films were cut into 25.4 mm x 101.6 mm strips for testing, and the thickness of each strip was measured to accurately calculate the cross-sectional areas. The grip separation was 50.8 mm, using flat rubber grips. Tests were run at a rate of 5 mm / minute using a 5 kN load cell. All data were recorded and processed using Instron's Bluehill 2 software, v. 2.21. The film's nominal stress was reported as tensile stress, TS:

$$TS = \frac{F}{A_c}$$

where F is the pound-force (lbf) applied to the film at break, and A_c is the cross-sectional area of the film (in²). Final TS was reported in MPa units. Percent elongation at break, %E, was calculated as:

$$\%E = \left(\frac{l_B - l_i}{l_i}\right) \times 100\%$$

where l_B is the length at break and l_i is the initial length. Five strips were analyzed for each film replicate. Data resulting from strips that tore prematurely or had imperfections from film casting were omitted in the data analysis and another sample was measured.

3.4.2. Water Vapor Permeability

WVP from WVTR was measured using a Permatran W model 3/34 (Mocon, Minneapolis, MN) according to ASTM F1249-13, "Standard Test Method for Water Vapor Transmission Rate Through Plastic Film and Sheeting Using a Modulated Infrared Sensor" (ASTM, 2013). The instrument was calibrated using an NIST traceable certified WVTR calibration film provided by Mocon. Films were masked with aluminum foil, reducing the test area to 3.14 cm^2 . Film thickness was measured for every sample to ensure accurate permeability calculations. The nitrogen carrier gas flow rate was 100 standard cubic centimeters per minute (SCCM). Permeation testing conditions were 23 ± 0.1 °C and 50.0 ± 0.1 % RH. The film was conditioned for 1 h, with testing cycling every 30 min. Two measurements were recorded for each film replicate. After the WVTR reached the steady state, the final three values were averaged to calculate WVP as follows:

$$WVP = \frac{WVTR \cdot l}{\Delta p}$$

where l is the film thickness (mm) and Δp is the water vapor partial pressure gradient across the film (2.81 kPa) (CRC, 2019).

3.4.3. Oxygen Permeability

OP was calculated from the oxygen transmission rate (OTR) which was obtained using an OxTran model 2/22 (Mocon, Minneapolis, MN) according to ASTM standard D3985-17 "Standard Test Method for Oxygen Gas Transmission Rate Through Plastic Film and Sheeting Using a Coulometric Detector" (ASTM, 2017). This instrument was standardized using an NIST traceable certified OTR reference film provided by Mocon. Films were prepared using the same technique as for WVP. Oxygen concentration was 100% with a 100 SCCM flow rate. Film conditions were $23^{\circ}\text{C} \pm 0.1^{\circ}\text{C}$ and $50.0 \pm 1.0\%$ RH. Films were conditioned for 2 h, and measurements were recorded every 30 min. Two measurements were recorded for each film replicate. Once OTR reached the steady state, the final three values were averaged and used to calculate OP:

$$OP = \frac{OTR \cdot l}{\Delta p}$$

where l is the film thickness (mm) and Δp is the partial pressure gradient of oxygen across the film (97.4 \pm 1.8 kPa, the measured atomospheric pressure).

3.5. Film Characterization

3.5.1. Ultra-violet Light Absorbance

Absorbance was measured using a Shimadzu UV-1800 UV-Vis Spectrophotometer (Kyoto, Japan). Films were placed in a spring-loaded film sample holder, and absorbance was measured from 190 to 300 nm at 1 nm sampling intervals at medium speed. Spectra were analyzed using UVProbe software v.2.42.

3.5.2. X-Ray Diffraction

XRD patterns were obtained using a D8 DaVinci diffractometer (Bruker, Billerica, MA) with the Cu X-ray radiation operating at 40kV and 40mA. Film samples were cut into strips and mounted in a PVMA sample holder. Peak intensities were counted every 0.02° at a sweep rate of $1.2^{\circ} 2\theta \text{ min}^{-1}$, with the samples being rotated at $5^{\circ} \text{ min}^{-1}$.

3.5.3. Microstructure

Film surface and cross-sectional microstructure was investigated using a scanning electron microscope (SEM) model JSM-6610 (JOEL USA, Peapody, MA). Samples were dried in a desiccator, cut, and mounted on aluminum stubs using double-sided carbon tape with the casting pan side down. Cross-sectional samples were naturally fractured and mounted on edge. The films were sputter coated with gold and analyzed at 12kV under X500 magnification.

3.5.4. Thermogravimetric Analysis

TGA was performed using a TGA model Q50 (TA Instruments, New Castle, DE). This instrument's temperature sensor was calibrated using nickel and alumel, and the balance was verified using standard weights. Each film formulation was analyzed as well as the individual film components including WPI, xylan, glycerol, and TG. Samples weighing 5 μg were heated from 10.00°C to 600.00°C at a rate of 10.00°C min⁻¹. TGA was performed once per film formulation or component.

3.5.5. Differential Scanning Calorimetry

A DSC Q100 (TA Instruments, New Castle, DE) was used to assess all film formulations as well as WPI and xylan. The instrument was calibrated using indium calibration standards. Aliquots of 5 μg were sealed in hermetic aluminum pans and heated from 10°C to 210°C at a rate of 10.00°C min⁻¹. DSC was performed once per film formulation.

3.6. Statistical Analysis

Each film formulation was replicated three times, and each replicate was tested three times unless specified otherwise. All statistical analyses were performed using R Studio v. 3.6.1. Two-way analysis of variance (ANOVA) was used to evaluate differences within each testing parameter. Significance was determined using Tukey's multiple range test with the criteria $p \le 0.05$. Student's *t*-test was used to evaluate the effect of treatments with and without TG at $p \le 0.05$.

4. RESULTS & DISCUSSION

4.1 Film Formulation

To ensure consistency in materials across film formulations, the same lot was used for each raw material component. Films produced were smooth, flexible, and homogeneous, containing no apparent bubbles or cracks. WPI films with and without TG were transparent. Films with higher levels of xylan became increasingly translucent. Xylan addition also produced a yellow tint to the otherwise colorless WPI films. The specific film forming process was derived from preliminary studies detailed in Appendix B. Initially, when sorbitol was used as a plasticizer, white, opaque patches began to form on the film surface presumably from the crystallization of sorbitol, as has been previously reported (Krogars et al., 2003). Preliminary experiments also produced tacky films with a WPI:glycerol ratio of 1:1. Glycerol-containing films can become sticky if the concentration is too high (Ramos et al., 2013), so the amount of plasticizer was reduced to a 3:1 ratio which produced dry-to-the-touch films that were still flexible. The enzymatic action of TG increased FFS viscosity as seen in other studies (Schmid et al., 2014). However, at a protein concentration at 5% (w/w) FFS was sufficiently dilute for adequate degassing and proper casting.

4.2 Film Description

All WPI film formulations were of uniform thickness (Table 5). There was no significant difference between the control and films containing xylan, with thicknesses ranging from 0.079 - 0.089 mm (p ≤ 0.05). WPI-TG and WPI-Xy40-TG films were significantly thicker at 0.106 and 0.094 mm, respectively (p ≤ 0.05). Increase thickness for films prepared with TG has been associated with increased isopeptide bond formation (Porta et al., 2011).

Table 5: Thickness, % moisture content, and density of whey protein isolate (WPI) films prepared with xylan (Xy) at 10 to 40 g Xy/100 g WPI and transglutaminase (TG)

Sample	Thickness (mm)	Moisture Content (%)	Density (g/cm ³)
WPI-TG	0.106 ± 0.001 °*	12.90 ± 3.04	1.06 ± 0.11 ^{b*}
WPI	0.084 ± 0.006^{ab}	14.74 ± 3.03	$1.39\pm0.03^{\rm c}$
WPI-Xy10	0.086 ± 0.003^{ab}	17.79 ± 0.84	0.94 ± 0.03^{ab}
WPI-Xy20	0.089 ± 0.001^{ab}	13.40 ± 2.42	$1.09\pm0.05^{\mathrm{b}}$
WPI-Xy30	0.085 ± 0.008^{ab}	12.43 ± 1.69	0.87 ± 0.06^{ab}
WPI-Xy40	0.079 ± 0.006^a	14.99 ± 0.95	0.84 ± 0.08^a
WPI-Xy40-TG	0.094 ± 0.006^{bc} *	13.03 ± 0.11	$1.62 \pm 0.14^{d*}$

Data corresponds to mean values and standard deviations of 3 replications

For each parameter, different lowercase letters show significant difference (p < 0.05)

Another explanation could be the increase in solids per 50 mL of pipetted FFS during casting. The TG formulation contained 90 – 99% maltodextrin in addition to the enzyme, according to the specification sheet provided by Ajinomoto.

Percent MC was not significantly different between any film formulations, with values ranging from 12.43 - 17.79% (p ≤ 0.05). This range is similar to films produced by Ramos et al. (2013) containing WPI and 40% glycerol that had an average of 15.1% MC. Films with increased polymer formation normally have a reduced number of active binding sites (hydroxyl groups), leading to less water binding (Cheng et al., 2008). No conclusions could be drawn from this study regarding polymer formation, as the standard deviation was large, possibly due to thickness variation in samples used to calculate % MC.

Film density is one indicator of how well components pack together, which relates to the intermolecular interactions in composite films. Formulations prepared with xylan without TG had a significantly lower density than the control ($p \le 0.05$). In comparing the control film containing only WPI to the enzymatically cross-linked WPI film, the density decreased from 1.39 to 1.06 g/cm³. The 40 g xylan/100 g WPI film increased in density with TG treatment from 0.84 to 1.62 g/cm³, the highest density in any film.

^{*}significant difference with the addition of TG (p < 0.05)

4.3 Color

Edible film color is an important part of application, as it may influence consumer perception of the product being packaged. The Beechwood xylan stock solution was brown, with dilute amounts imparting a yellow tint to the films (Figure 7). The addition of xylan significantly changed the color of WPI-Xy20 – 40 and WPI-Xy40-TG films, as compared to the control using ΔE (Table 6) (p \leq 0.05). YI increased as xylan increased up to 30 g/100 g WPI. WPI-Xy30, WPI- Xy40, and WPI-Xy40-TG films were not significantly different from one another (p > 0.05). The addition of TG significantly increased YI for the WPI film, but not for the WPI-Xy40 formulation (p > 0.05). The yellowing of whey protein films over time is an established drawback to their use packaging materials, identified in studies on film aging performed by Trezza & Krochta (2000). This color change is product of the Maillard reaction between lysine residues in the protein and residual lactose. The yellow appearance due to xylan addition could enhance the natural yellowing of WPI films.

The brown color of xylan is a product of processing HC with lignin impurities. The level of impurities varies based on different HC sources and extraction methods, with high amounts of lignin having been known to darken HC films (Sabiha-Hanim & Siti-Norsafurah, 2012). Lignin content can be quantitatively analyzed in solution by measuring the absorbance at 205 or 280 nm (Skulcova et al., 2017). The spectra obtained from 200 – 300 nm (Figure 8) showed absorbances above the detection limit at 205 and 280nm for all films. The signal registers as absorbance on the instrument but may be a result of light scattering by the films, which were all translucent to some degree. A decrease in absorbance was observed from 240 – 270 nm for all films. However, the magnitude cannot be used to compare spectra as there were variations in film thickness.



Figure 7: Yellowing of whey protein isolate (WPI) films prepared with xylan(Xy) from 10 to 40 g Xy/100 g WPI and transglutaminase (TG)

Table 6: Color changes in whey protein isolate (WPI) films prepared with xylan (Xy) from 10 to 40 g Xy/100 g WPI and transglutaminase (TG)

Sample	L	a	b	ΔΕ	YI
WPI-TG	$92.47\pm0.05^{\rm c}$	-1.14 ± 0.06^{ab} *	6.03 ± 0.10^{a} *	0.70 ± 0.11^a	$9.31 \pm 0.15^{a*}$
WPI	92.30 ± 0.09^{c}	$\text{-}0.77 \pm 0.04^{\mathrm{d}}$	$5.46\pm0.17^{\rm a}$		8.45 ± 0.26^a
WPI-Xy10	92.18 ± 0.25^{c}	$\text{-}1.04 \pm 0.03^{bc}$	7.35 ± 0.36^{b}	$1.92\pm0.37^{\rm a}$	11.39 ± 0.58^{b}
WPI-Xy20	91.83 ± 0.50^{bc}	$\text{-}1.01 \pm 0.05^{bc}$	9.00 ± 0.68^{c}	3.59 ± 0.75^{b}	14.00 ± 1.14^{c}
WPI-Xy30	91.02 ± 0.68^{ab}	$\text{-}0.98 \pm 0.05^{c}$	$10.35\pm0.57^{\mathrm{d}}$	5.07 ± 0.73^{c}	16.25 ± 1.02^{d}
WPI-Xy40	90.76 ± 0.23^a	$\text{-}1.07 \pm 0.05^{bc}$	9.79 ± 0.33^{cd}	4.60 ± 0.39^{bc}	15.41 ± 0.56^{cd}
WPI-Xy40-TG	$90.22 \pm 0.15^{a} *$	$\text{-}1.24 \pm 0.06^{a} \text{*}$	10.06 ± 0.38^{cd}	5.07 ± 0.41^{c}	15.93 ± 0.63^{cd}

L, a, b: Hunter's Lab color values

 $[\]Delta E$: change in color from control film

YI: yellowness index

Data corresponds to mean values and standard deviations of 3 replications

For each parameter, different lowercase letters show significant difference (p < 0.05)

^{*}significant difference with the addition of TG (p < 0.05)

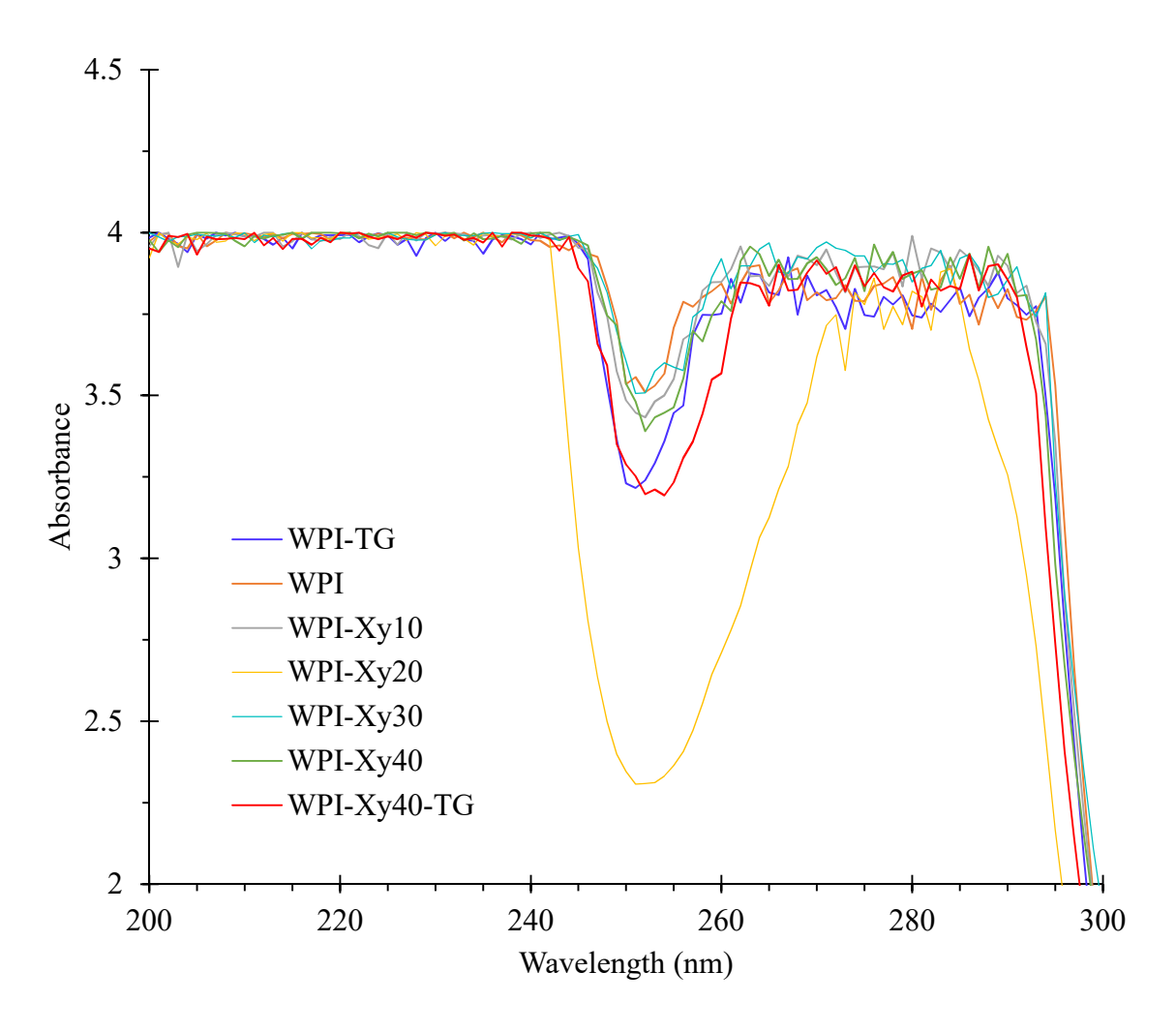


Figure 8: Absorbance of whey protein isolate (WPI) edible films prepared with xylan (Xy) and transglutaminase (TG) at 200 to 300 nm

^{*}Xy0 - Xy40 (TG) = increasing Xy content from 0 - 40 g Xy / 100g WPI, with and without TG

4.4. Properties Impacting Food Application

4.4.1. Water Vapor Permeability

The water vapor permeability of food packaging materials is partially responsible for controlling the microbiological growth that leads to food spoilage. WVP in WPI films decreased with the addition of xylan and TG (Figure 9, Table 7). Control films showed a WVP of 6.41 g mm/m² day kPa. The WVP decreased with increasing amounts of xylan, however only the WPI-Xy40 films were significantly different from the control with a permeation coefficient of 4.53 g mm/m² day kPa ($p \le 0.05$). Xylan has been shown to decrease WVP in protein films prepared from gluten, possibly due to their slightly lower solubility compared to protein (Kayserilioğlu et al., 2003). TG significantly reduced WVP by 37.2% in the WPI-only film and 14.1% in the 40 g xylan/100 g WPI film (p < 0.05). The WPI-Xy40-TG formulation provide the greatest moisture barrier, with a WVP of 3.89 g mm/m² day kPa. This effect has been observed in other PS and whey protein composite films. Jiang et. Al (2016) reported a lower WVP in TG cross-linked films of carboxymethylated chitosan and WPC, at ratios of 1:1 or lower. The decrease in WVP was less without the addition of TG (Jiang et al., 2016). A similar trend was observed in unmodified chitosan and whey protein films, where the addition of TG decreased WVP by 72% (Di Pierro et al., 2006).

Table 7: Mechanical and barrier properties (23°C, 50% RH) of whey protein isolate (WPI) edible films with xylan (Xy) and transglutaminase (TG)

Sample	Tensile stress (MPa)	Elongation at break (%)	WVP (g mm/m² day kPa)	OP (cc μm/m² day kPa)
WPI-TG	$8.25 \pm 0.32^{a*}$	$1.4\pm0.1^{a*}$	$4.02 \pm 0.23^{a*}$	11.96 ± 0.39 ^b *
WPI	$6.73\pm0.25^{\rm a}$	$12.5\pm3.1^{\rm c}$	$6.41\pm0.59^{\rm c}$	21.85 ± 0.76^{d}
WPI-Xy10	10.58 ± 1.56^{ab}	3.0 ± 0.8^{ab}	$6.27\pm0.49^{\rm c}$	20.76 ± 0.75^{d}
WPI-Xy20	11.89 ± 3.06^{abc}	1.9 ± 0.6^{ab}	5.60 ± 0.58^{bc}	16.22 ± 1.42^{c}
WPI-Xy30	15.58 ± 0.91^{bc}	2.2 ± 0.0^{ab}	6.29 ± 0.14^c	16.21 ± 0.75^{c}
WPI-Xy40	$8.38\pm1.67^{\rm a}$	3.2 ± 0.7^{ab}	4.53 ± 0.08^{ab}	11.31 ± 0.76^{b}
WPI-Xy40-TG	$15.96 \pm 3.14^{c*}$	5.8 ± 1.8^{b}	$3.89\pm0.27^{\mathrm{a}}$	7.32 ± 0.38^{a}

WVP = water vapor permeability

Data corresponds to mean values and standard deviations of 3 replications

For each parameter, different lowercase letters show significant difference (p < 0.05)

^{*} significant difference with the addition of TG (p < 0.05)

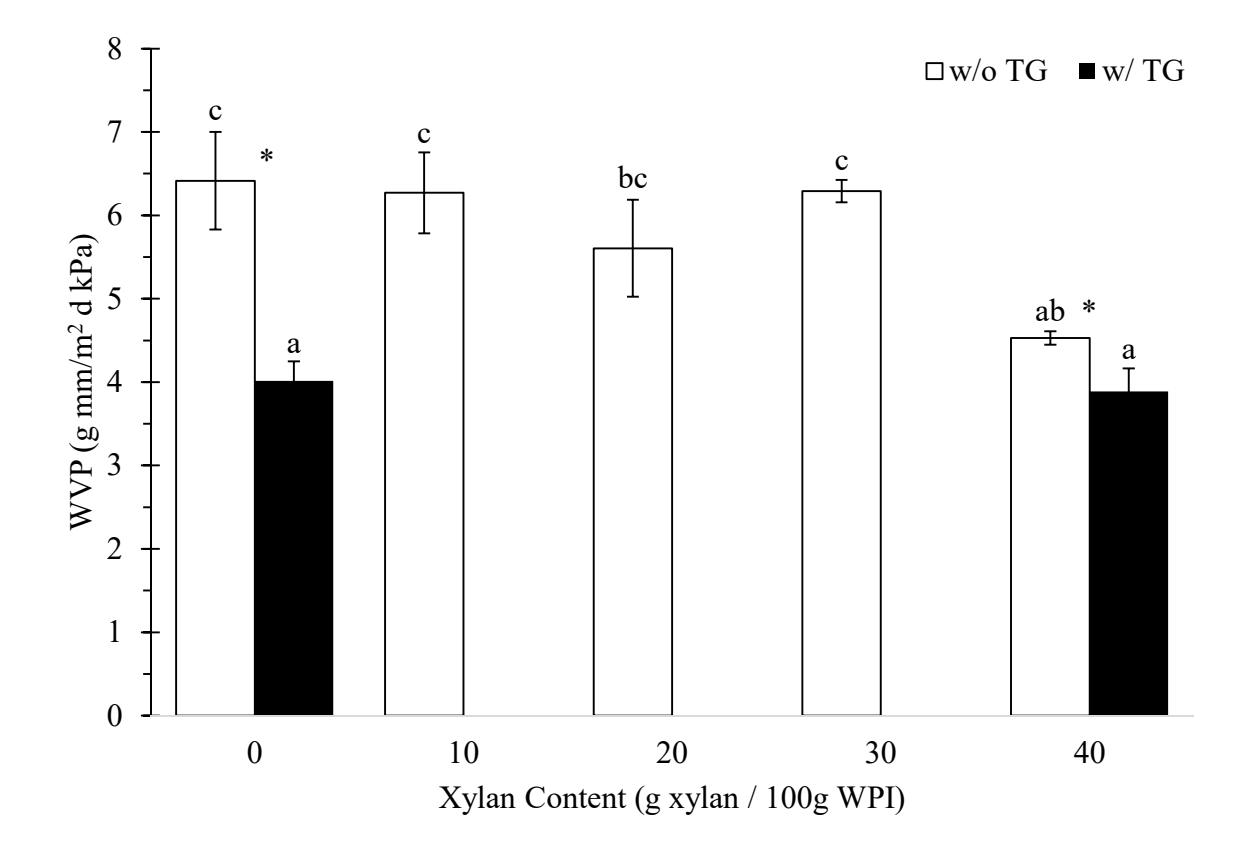


Figure 9: Water vapor permeability (WVP) coefficients for whey protein isolate (WPI) edible films as a function of xylan content and transglutaminase (TG)) (23°C, 50% RH) Different lowercase letters show significant difference (p < 0.05); * denotes significant difference with the addition of TG (p < 0.05).

OP = oxygen permeability

4.4.2. Oxygen Permeability

Lipid oxidation can produce rancid flavors and affect the quality of foods, so the amount of oxygen in contact with the food must be limited. Microbial degradation of food products can also be reduced by limiting oxygen. WPI films are already known to have excellent barrier properties to oxygen. This is due to the polar nature of the film, which has lower sorption and diffusion to the nonpolar oxygen gas molecule. Proteins have nonpolar regions, so oxygen permeability can be lowered by decreasing the protein to xylan ratio. The WPI control film had an OP of 21.85 cc μm/m² day kPa, with the addition of xylan significantly decreasing this value at concentrations at and above 20 g xylan/100 g WPI (p < 0.05) (Table 7, Figure 10). WPI-Xy40 films had an OP of 11.31 cc µm/m² day kPa, which was comparable to the WPI-TG film at 11.96 cc μm/m² day kPa. The effect of PS type on OP of WPI films is quite variable. One study showed decreases in OP for corn starch and sodium alginate, while methyl cellulose increased OP (Yoo & Krochta, 2011). The lowest OP occurred in the WPI-Xy40-TG film, reaching 7.32 cc µm/m² day kPa. This is similar to previous results for composite films containing chitosan and WPI, where a decrease from 20.6 cc μm/m² day kPa to 7.8 cc μm/m² day kPa was observed by only adding TG (Di Pierro et al., 2006).

4.4.3. Mechanical Properties

Mechanical strength and elasticity of packaging materials are not only important in protecting food products, but also in maintaining the integrity of the package's previously discussed barrier properties. The addition of xylan increased TS of WPI-only films from 6.73 MPa up to 15.58 MPa at 30g xylan / 100g WPI (Figure 11, Table 7). This trend did not continue for the WPI-Xy40 formulation, which had a TS of 8.38 MPa, suggesting a possible optimal xylan content for the TS of WPI films. A similar pattern was observed in WPI films containing oat

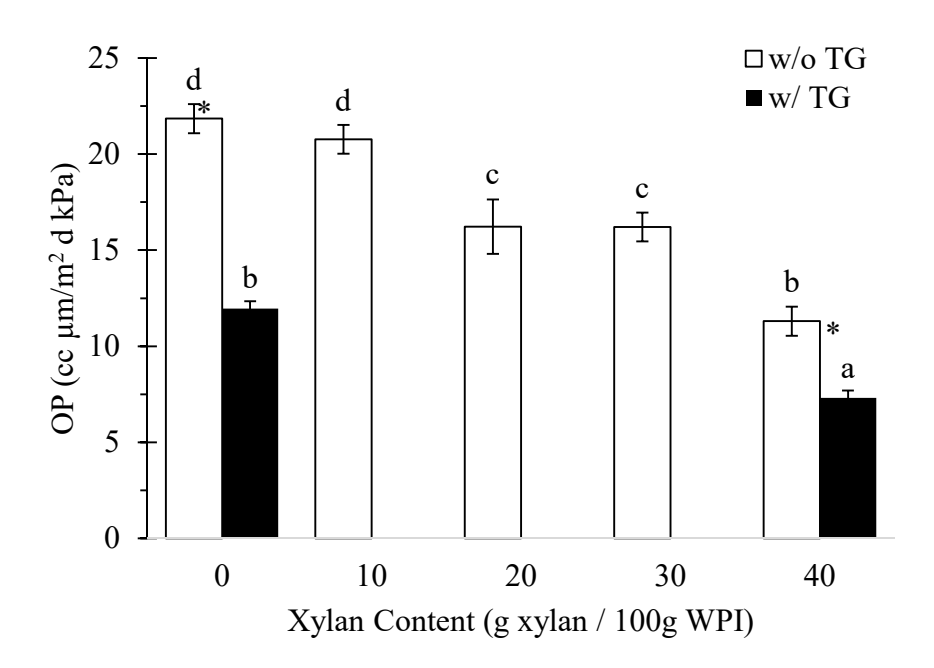


Figure 10: Oxygen permeability (OP) coefficients for whey protein isolate (WPI) edible films as a function of xylan content and transglutaminase (TG) (23°C, 50% RH)

Different lowercase letters show significant difference (p < 0.05);

The sign * denotes significant difference with the addition of TG (p < 0.05).

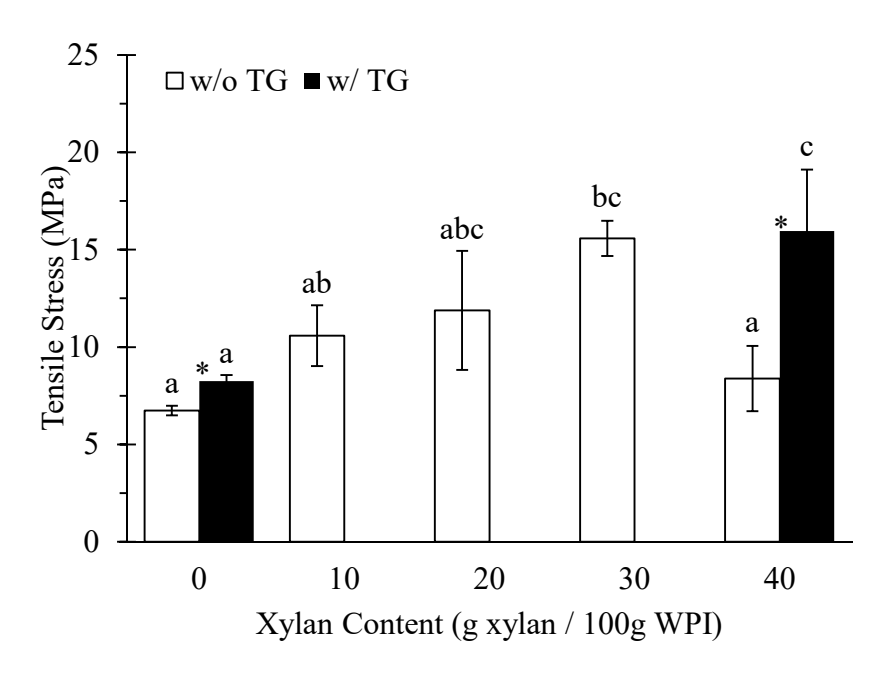


Figure 11: Tensile stress of whey protein isolate (WPI) edible films as a function of xylan content and transglutaminase (TG) treatment)

Different lowercase letters show significant difference (p < 0.05);

^{*}significant difference with the addition of TG (p < 0.05).

husk nanocellulose. The addition of PS increased TS up to 5% (w/w), with TS decreasing at 7.5% (w/w) (Qazanfarzadeh & Kadivar, 2016). The addition of TG significantly increased TS in both cases, with the highest TS observed in WPI-Xy40-TG films at 15.96 MPa. Increased covalent bonding associated with crosslinking was expected to improve TS, as mechanical properties are dependent on the distribution of inter- and intramolecular forces (Chambi & Grosso, 2006).

The effect of xylan addition on %E was the inverse of that seen for TS, with %E decreasing with increasing xylan (Figure 12). The %E decreased sharply from 12.5% in the WPI films to 1.9 – 3.2% in all WPI and xylan films. TG minimally affected the % E of WPI film at 1.4%. This pattern is caused by the same molecular forces that affect TS, as stronger films have less mobility, reducing their %E at break. The %E was significantly higher for WPI-Xy40-TG than for WPI-TG films which may be the result of increased mobility between the TG protein

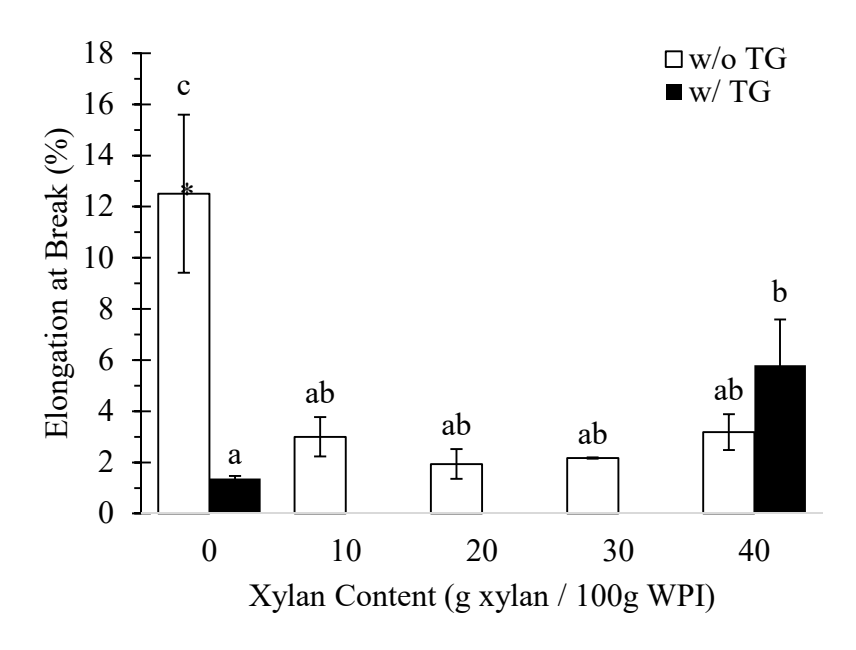


Figure 12: Percent Elongation at break of whey protein isolate (WPI) edible films as a function of xylan content and transglutaminase (TG)

Different lowercase letters show significant difference (p < 0.05);

The sign * denotes significant difference with the addition of TG (p < 0.05).

cross-links within regions of xylan. Overall, the %E values were very low for the composite films, and more flexible films could be produced by increasing the plasticizer concentration.

4.5. Film Characterization

4.5.1. Crystallinity

Cast biopolymer films do not have a uniform makeup due to imperfections in the casting surface and variations in thickness. As a result, the XRD analysis was not used to calculate % crystallinity, but rather to compare the presence or absence of crystalline regions by comparing peak locations and sharpness. WPI and WPI-TG films produced wide, dull peaks at around $2\theta =$ 8° and 19.5°, which have been reported for other WPI films (Aziz & Almasi, 2018) (Figure 13). These wide peaks indicate that the films had a lower degree of crystallization and were more amorphous in their molecular structure. As xylan content increased, a peak developed at $2\theta =$ 18.2° with increasing sharpness at higher xylan levels. This peak is indicative of a higher degree of short-range order in the otherwise amorphous structure of films (Carà et al., 2013). There was an apparent decrease in magnitude for the WPI-Xy40 film, which could be related to the observed decrease in TS since high levels of lignocellulose to will aggregate instead of remaining evenly dispersed (Qazanfarzadeh & Kadivar, 2016). The peak at $2\theta = 18.2^{\circ}$ returned to prominence for the WPI-Xy40-TG film, and this is also mirrored in the results seen for TS. The general pattern of increased crystallinity correlates well with the observed improved barrier properties for both water vapor and oxygen.

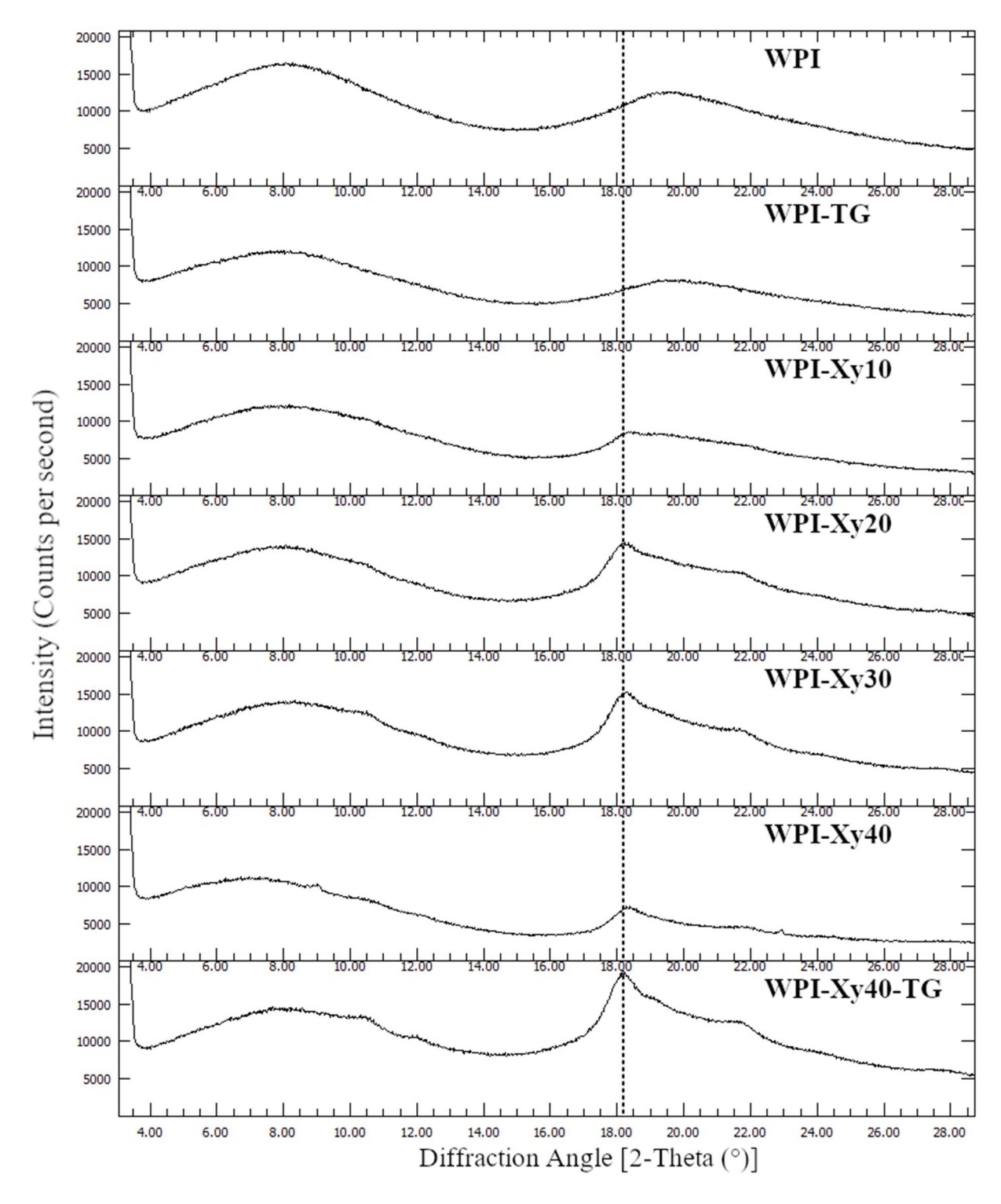


Figure 13: XRD analysis of whey protein isolate (WPI) films with xylan (Xy) and transglutaminase (TG)

^{*}Xy0 - Xy40 (TG) = increasing xylan content from 0 - 40 g Xy / 100g WPI, with and without TG

4.5.2. Microstructure

The film surface microstructure became increasingly heterogeneous with the addition of xylan (Figure 14). Both WPI and WPI-TG films had smooth and homogeneous surfaces, with very few imperfections. The addition of xylan produced organized, circular structures on the film surface. These structures increased in size with xylan content. WPI-Xy10, WPI-Xy20, and WPI-Xy30 exhibited circles with maximum size of about 12, 24, and 37 µm, respectively. This organization decreased in sharpness for WPI-Xy40. If these structures indicate unincorporated, higher crystallinity xylan regions, the disappearance of the structures in WPI-Xy40 films could explain the decrease in mechanical strength previously observed. WPI-Xy40-TG films were heterogeneous, with some regions lacking any definition and others with circular structures up to 30 µm in diameter. These structures appear to be depressions, as opposed to the almost bubble-like appearance seen in non-TG containing xylan films. This could be a product of a tighter structure from the cross-linking of proteins, supported by the high density observed for this film treatment.

Film cross-sectional images show the dispersion of the globular structures throughout the film (Figure 15). In this side view, the circular structures appear as horizontal slits in the film, with fractures connecting adjacent structures. These globules are likely not air bubbles but rather contained regions of separated xylan. WPI-Xy40 films exhibited two distinct regions of differing xylan density which may be a product of xylan aggregation, leading to a decreased evenness of dispersion as seen in other WPI/PS films at high levels of PS (Qazanfarzadeh & Kadivar, 2016). WPI-Xy40-TG films exhibited less fracturing between organized regions, possibly due to increased covalent bonding by TG.

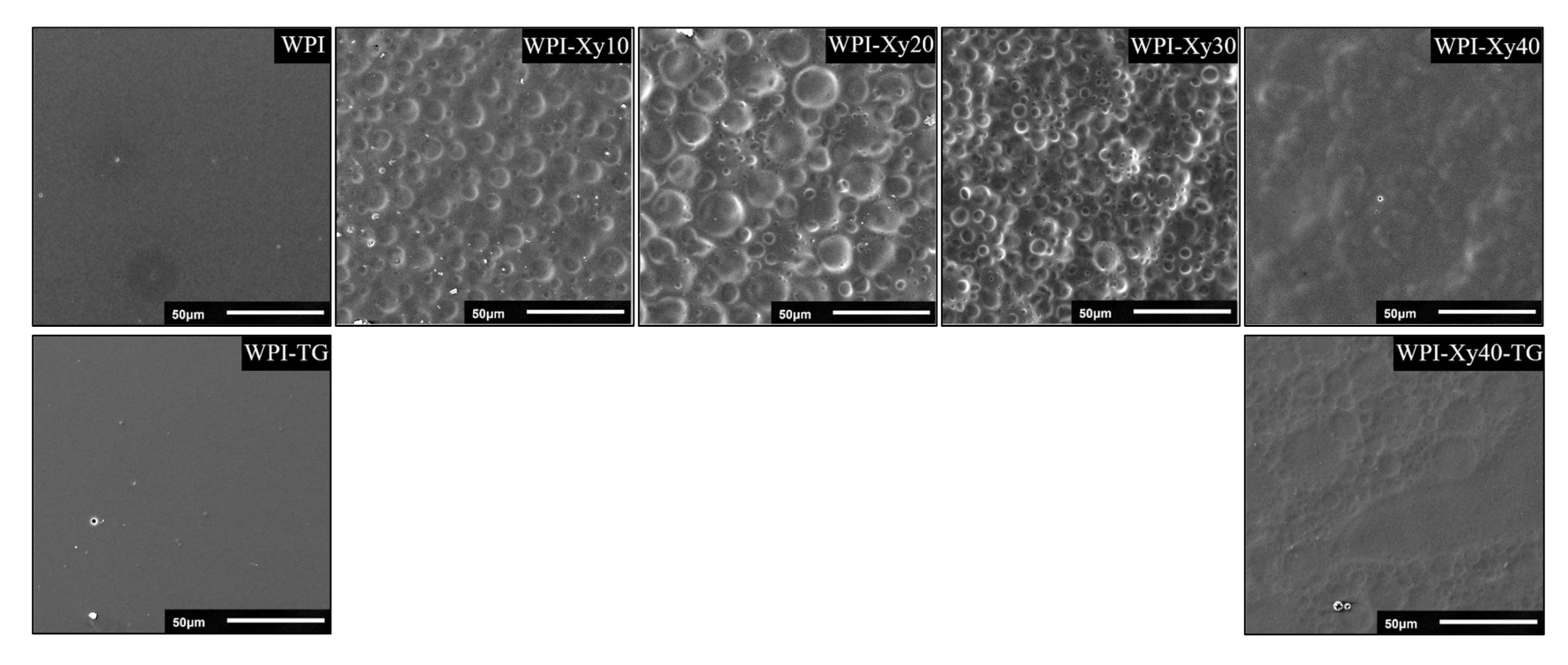


Figure 14: Surface microstructure of whey protein isolate (WPI) films prepared with xylan (Xy) and transglutaminase (TG). Images captured through SEM at 500x magnification

Xy0 – Xy40 (TG) = increasing xylan content from 0 – 40 g Xy / 100g WPI, with and without TG

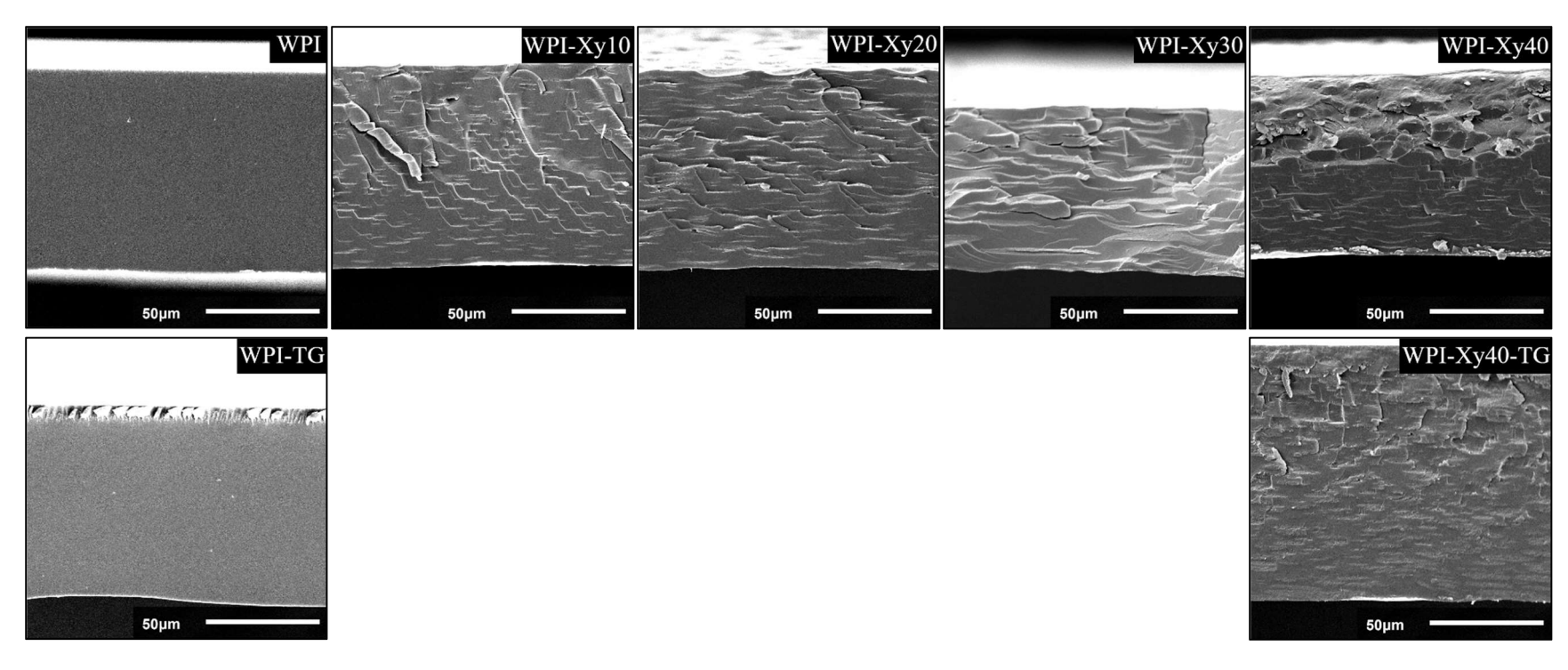


Figure 15: Microstructure of fractured film edge of whey protein isolate (WPI) films prepared with xylan (Xy) and transglutaminase (TG). Images captured through SEM at 500x magnification Xy0 - Xy40 (TG) = increasing xylan content from 0 - 40 g Xy / 100g WPI, with and without TG

4.5.3. Differential Scanning Calorimetry

The temperature at which a polymer transitions from a crystalline to an amorphous organization relates to the strength of the intra- and inter-molecular polymer bonds. This melting temperature is important for films when determining possible processing conditions, like heat sealing or extrusion. The addition of xylan to WPI films increased the onset temperature and melting temperature, T_m , for all treatments (Table 8). WPI-Xy20 had the highest T_m , increasing from 121 to 166°C over the control WPI film. The 30 and 40 g xylan/ 100 g WPI films showed a slightly lower increase in T_m over the control films. A higher T_m can be an indicator of good miscibility (Chakravartula et al., 2019), so it is possible that xylan was less evenly dispersed at these higher concentrations as also seen in –the SEM micrographs with xylan aggregating at higher levels.

Table 8: DSC analysis from melting point curves of whey protein isolate (WPI) films prepared with xylan (Xy) and transglutaminase (TG)

Sample	Onset temperature (°C)	Melting point, T_m (°C)	Reaction Heat, ΔH (J/g)
WPI-TG	109	140	170.3
WPI	68	121	123.8
WPI-Xy10	126	157	122.2
WPI-Xy20	130	166	102.7
WPI-Xy30	76	127	165.5
WPI-Xy40	107	140	122.6
WPI-Xy40-TG	99	135	182.7

Xy0 - Xy40 (TG) = increasing xylan content from 0 - 40 g Xy / 100g WPI, with and without TG

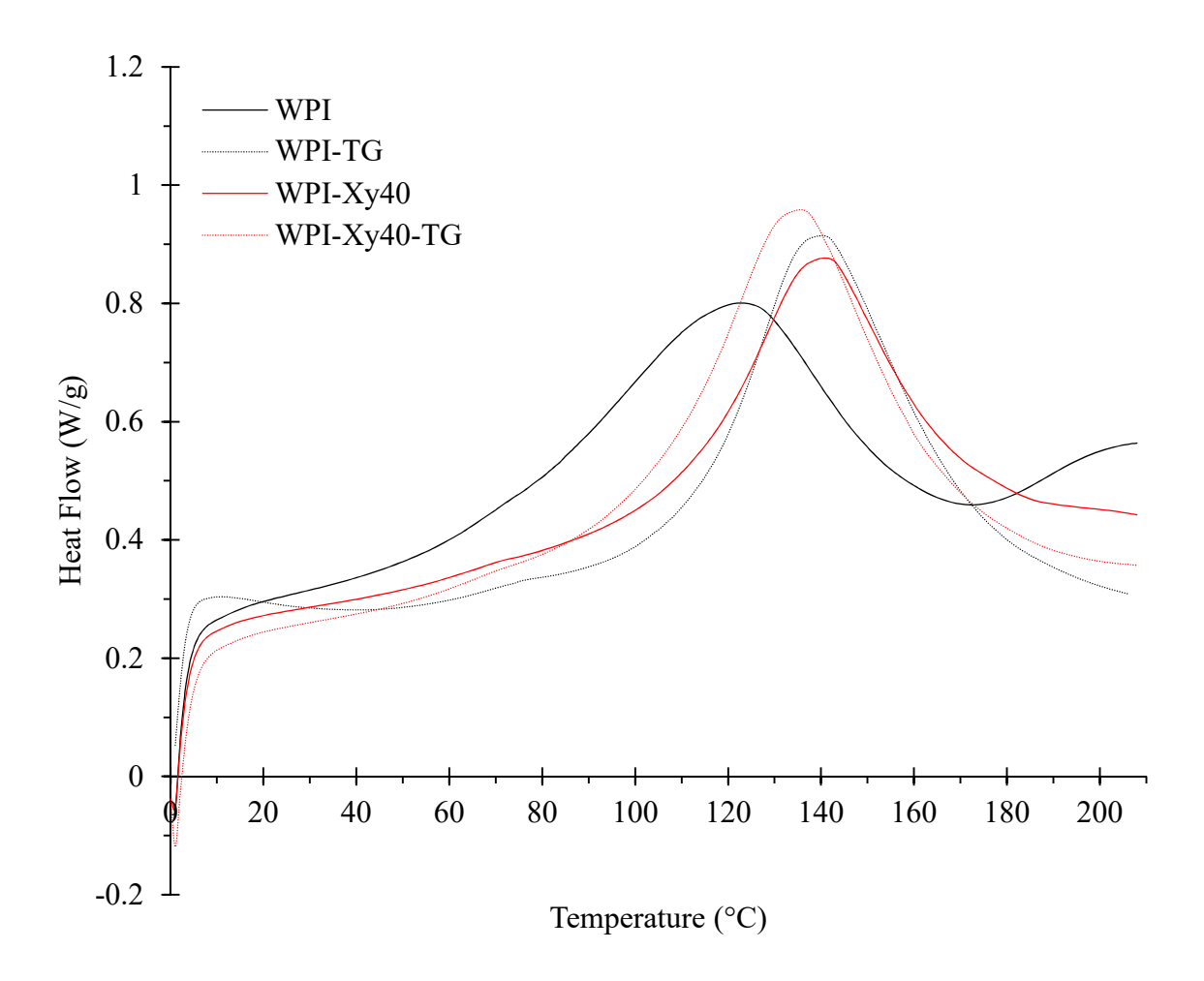


Figure 16: DSC profiles of whey protein isolate (WPI) films prepared with 40 g xylan / 100 g WPI (WPI-Xy40) and transglutaminase (TG)

The addition of TG increased the reaction heat, ΔH , by 46.5 J/g in WPI films and 60.1 J/g in WPI-Xy40 films (Figure 16). This higher ΔH indicates more strongly bonded polymers, as more energy is required for the transition from crystalline to amorphous form. TG cross-linking increased T_m in WPI films, but not in WPI-Xy40 films. This could be the result of poorer miscibility in the WPI-Xy40-TG film, which had a very heterogeneous surface microstructure. Cross-linking agents have been shown to improve thermal properties of WPI films by increasing transition temperatures and ΔH (Quan et al., 2018).

4.5.4. Thermogravimetric Analysis

The thermal stability of each film formulation was evaluated using TGA to identify new interactions including xylan-WPI molecular interactions beyond the simple mixture formation. The TGA curves for WPI films consisted of three main regions of thermal decomposition: 40 – 135°C, 135 – 450°C, and 450 – 560°C (Table 9). The T_{max} in the first region ranged from 71 – 97°C, and is thought to be the water loss (Chakravartula et al., 2019). The TG-containing films had a higher T_{max} than their counterparts, which may have been the result of water and glycerol being trapped in a more firmly linked protein network.

The second region, 135 – 450°C, was the bulk of material decomposition. Other WPI film studies have suggested that this region accounts for the degradation of WPI proteins and glycerol (Kadam et al., 2013). The WPI control film had a pronounced peak shoulder at 210°C and a main peak at 307°C (Figure 17). This shoulder peak decreased in prominence with increasing levels of xylan and is the result of a two-phase breakdown in this temperature range. The addition of TG completely removed the shoulder, with decomposition occurring at an even rate in these samples.

Table 9: TGA analysis of whey protein isolate (WPI) films prepared with increasing xylan (Xy) content and transglutaminase (TG)

Sample	T _{max} (°C) of derivative curve over 40 – 135°C	T _{max} (°C) of derivative curve over 135 – 450°C	Weight loss (%) Over 450 – 560°C
WPI-TG	97	303	26.08
WPI	71	307*	5.288
WPI-Xy10	80	316*	27.18
WPI-Xy20	74	309*	29.52
WPI-Xy30	77	308*	26.77
WPI-Xy40	78	306*	25.5
WPI-Xy40-TG	93	306	25.05

Xy0 - Xy40 (TG) = increasing xylan content from 0 - 40 g Xy / 100g WPI, with and without TG

^{*} indicates a second peak or shoulder was present on the derivative curve within the given temperature range.

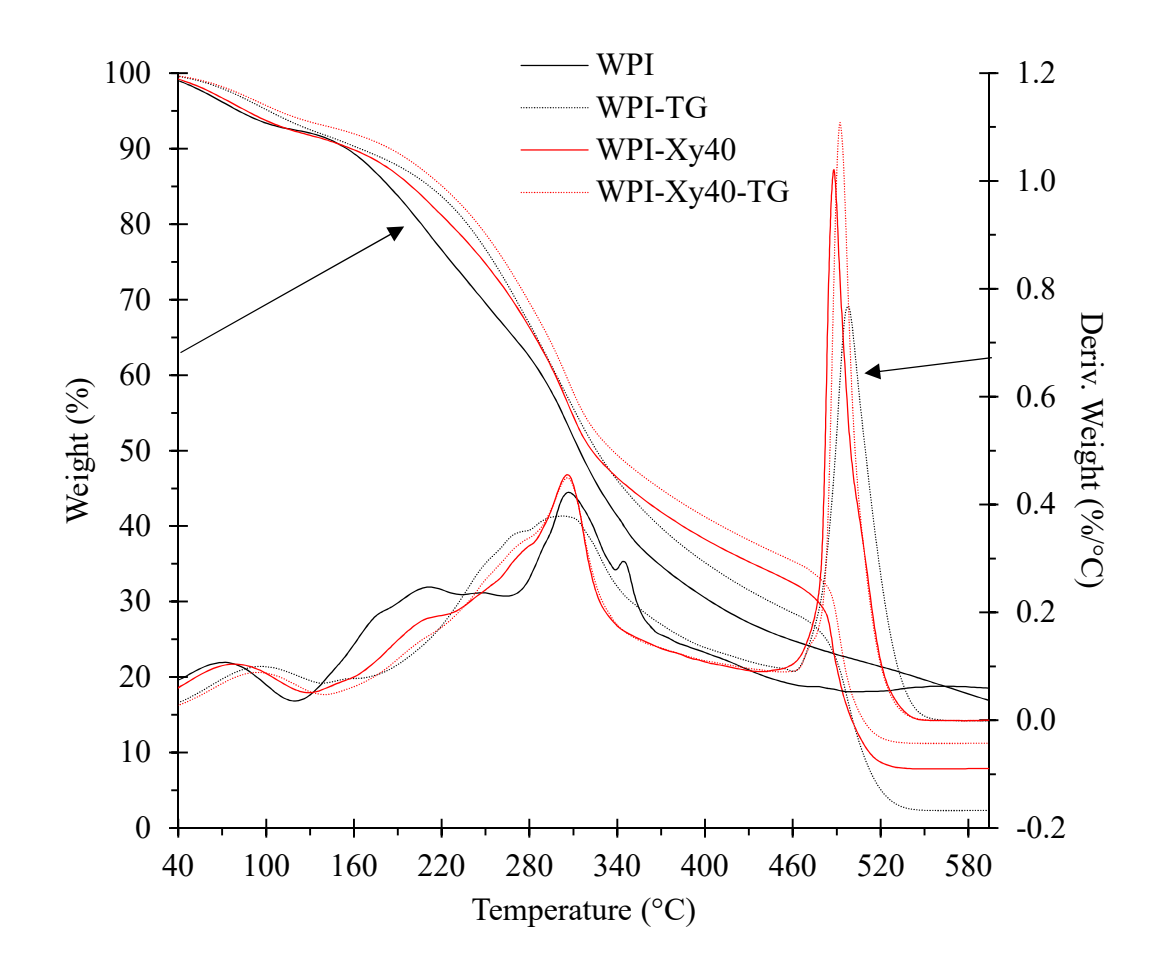


Figure 17: TGA profiles of whey protein isolate (WPI) films treated with 40 g xylan / 100g WPI (WPI-Xy40) and transglutaminase (TG)

Degradation over the 450 - 560°C region was between 25.05 and 29.52% weight loss for all WPI films that were treated with xylan and/or TG. The WPI-only film exhibited a 5.28% reduction in weight, meaning that the film components did not completely decompose under 560°C, with some residues remaining.

5. CONCLUSIONS

- The yellowness index significantly increased with increasing amounts of xylan up to 30 g xylan / 100 g WPI, at which point no difference in yellowness was observed. The addition of TG increased yellowness in WPI-only films but not in WPI-Xy40 films.
- WVP decreased significantly with the addition of TG as well as xylan at 40 g xylan / 100 g WPI.
- OP decreased significantly with the addition of TG, as well as xylan at levels from 20 –
 40 g xylan / 100 g WPI.
- TS increased significantly with the addition of TG and xylan at 30 g xylan / 100 g WPI.
 Percent elongation at break decreased significantly in all film formulations
- DSC testing showed an increase in melting temperature for all films compared to the control.
- TGA showed the elimination of a two-stage protein degradation in the 135 450°C region with the addition of TG. Additionally, film degradation from 450 560°C occurred in all films except the control.
- Physical characterization through XRD analysis indicated increased crystalline regions
 with increasing xylan. Observations of film microstructure indicated organized circular
 structures with increasing amount of xylan.

6. RECOMMENDATIONS

This study produced WPI films with improved barrier and mechanical properties through the addition of xylan. Future studies may look at further improving other properties, such as % elongation at break, through the addition of more plasticizer. As microstructure analysis revealed organized regions when xylan was added, another future study might investigate different methods of combining film components: extending the amount of homogenization that occurs, different drying and curing methods, or the use of sonication on the film forming solution. Due to material management, TG was only used on the control and the best performing xylan concentration. It would perhaps be beneficial to investigate its effect on all xylan levels in the WPI films.

Application is an important part of edible films which can be altered though the use of additives in addition to the xylan. This may include thyme or rosemary extracts, which are natural antimicrobials. Antioxidants may also be used in future film studies. Finally, it is important to note that edible films will be consumed at some point, so sensory studies may be beneficial to an analysis of xylan films. Nutritional studies may also be considered, as xylan has been described as an "unconventional source of dietary fiber" (Olson et al., 1983).

APPENDICES

APPENDIX A: Material Specs

Table 10: Xylan compositional analysis from Megazyme's specification sheet

	Pol	ysaccharide Con	de Content Overall Xy		ccharide Content Overall Xylan Composition		osition
Properties	Xylose, %	Glucuronic acid, %	Other sugars, %	Protein, %	Ash, %	Moisture, %	
Xylan (Beechwood) Lot 141201	82.3	12.8	4.9	0.2	4.7	4.1	

Table 11: Whey protein isolate compositional specifications from Grande Ingredients Group

Chemical	Specification
Protein % (DB)	90.0 Min
Moisture %	6.0 Max
Carbohydrate %	6.5 Max
Fat %	2.0 Max
Ash %	3.5 Max
pH 10% at 20°C	5.8-6.8

Table 12: Typical amino acid profile of whey protein isolate provided by Grande Ingredients Group (grams amino acid per 100 grams protein)

Amino Acid	% of Protein	Amino Acid	% of Protein
Alanine	5.05	Lysine	9.38
Arginine	2.00	Methionine	2.09
Aspartic Acid	10.98	Phenylalanine	2.88
Cysteine	2.17	Proline	6
Glutamic Acid	17.36	Serine	4.57
Glycine	1.58	Threonine	7.01
Histidine	1.64	Tryptophan	1.93
Isoleucine	6.56	Tyrosine	2.72
Leucine	10.35	Valine	5.73

APPENDIX B: Preliminary Experiments

Several preliminary experiments were performed to produce a standalone film that would be testable in the packaging lab. Their preparation and notable characteristics are detailed in this appendix.

Trial 1

Film Formation:

A 10% (w/w) WPI stock solution was prepared by dissolving WPI in a 100 mM sodium phosphate buffer of pH 6.0. The stock solution was heated while stirring on a hot plate to 65°C for 10 minutes. After cooling the FFS to room temperature, the treatments were added according to 14 experimental designs detailed in Table 13. Sorbitol and glycerol were added in varying amounts as film plasticizers. TG was used at an activity of 30 units of activity per gram for multiple preparations. The treatments were mixed in 50mL conical tubes and 20 mL of each FFS was cast in 100mm petri dishes and dried at room temperature and humidity. After 24 hours of drying, the films were qualitatively analyzed (Figure 18).

Observations:

All films were completely shattered, an indication that the amount of plasticizer was insufficient. The degree of shattering did differ, which informed the compositional changes in the next trial. No distinct difference was observed between the sorbitol or glycerol films, and the size of the fragments increased with increasing plasticizer amount. The addition of TG to the films was a vast improvement with far fewer cracks. This trial suggested that the amount of plasticizer should be increased, and that TG improves film crosslinking.

Table 13: Preliminary experiment (1 of 5) treatment formulations for whey protein isolate (WPI) crosslinked with transglutaminase (TG)

Note: Gly = glycerol; Sor = sorbitol

Film#	10% WPI Stock Solution (mL)	WPI : Plasticizer (ratio)	TG (IU)	Phosphate Buffer (mL)
1	20			
2	10	20:1 Gly		10
3	10	10:1 Gly		10
4	10	6.7: 1 Gly		10
5	10	20:1 Gly	30	10
6	10	10:1 Gly	30	10
7	10	6.7: 1 Gly	30	10
8	10	20:1 Sor		10
9	10	10:1 Sor		10
10	10	6.7: 1 Sor		10
11	10	20:1 Sor	30	10
12	10	10:1 Sor	30	10
13	10	6.7: 1 Sor	30	10
14	10		30	10



Figure 18: Preliminary experiment results (1 of 5) for whey protein isolate (WPI) standalone films crosslinked with transglutaminase (TG)

Note: Exact component ratios for treatments 1-14 are detailed in Table 13

Trial 2

Film Formation:

Film preparation was performed according to the methods outlined in Trial 1. The WPI stock solution concentration was increased from 10% (w/w) to 20% (w/w). An 8% w/w xylan stock solution was prepared by dissolving xylan in a 100mM sodium phosphate buffer of pH 6.0. This solution was added to the cooled stock solution of WPI in several treatments. The exact relative amounts in the film forming solutions are detailed in Table 14. After 24 hours of drying, the films were qualitatively analyzed (Figure 19).

Observations:

Film integrity improved from the previous trial, observed as less shattering. The addition of TG increased opacity in films, and the addition of xylan produced a brown tint to the otherwise colorless films. The highest quality film (treatment #11) contained the highest levels of plasticizer, xylan, and TG. Treatment #12, which had a 1:1 WPI to sorbitol ratio, was shattered and the pieces were immovable – the gummy material was attached to the petri dish.

Table 14: Preliminary experiment (2 of 5) treatment formulations for whey protein isolate (WPI) and xylan composite films crosslinked with transglutaminase (TG)

	20% WPI Stock	WPI : Sorbitol	TG	WPI : Xylan	Phosphate
Film#	Solution (mL)	(ratio)	(IU)	(ratio)	Buffer (mL)
1	10				10
2	10	5:1			10
3	10	3.3:1			10
4	10		30		10
5	10		60		10
6	10			5:1	10
7	10			3.3:1	10
8	10	3.3:1	60		10
9	10	3.3:1		3.3:1	10
10	10		60	3.3:1	10
11	10	3.3:1	60	3.3:1	10
12	5	1:1	30		15

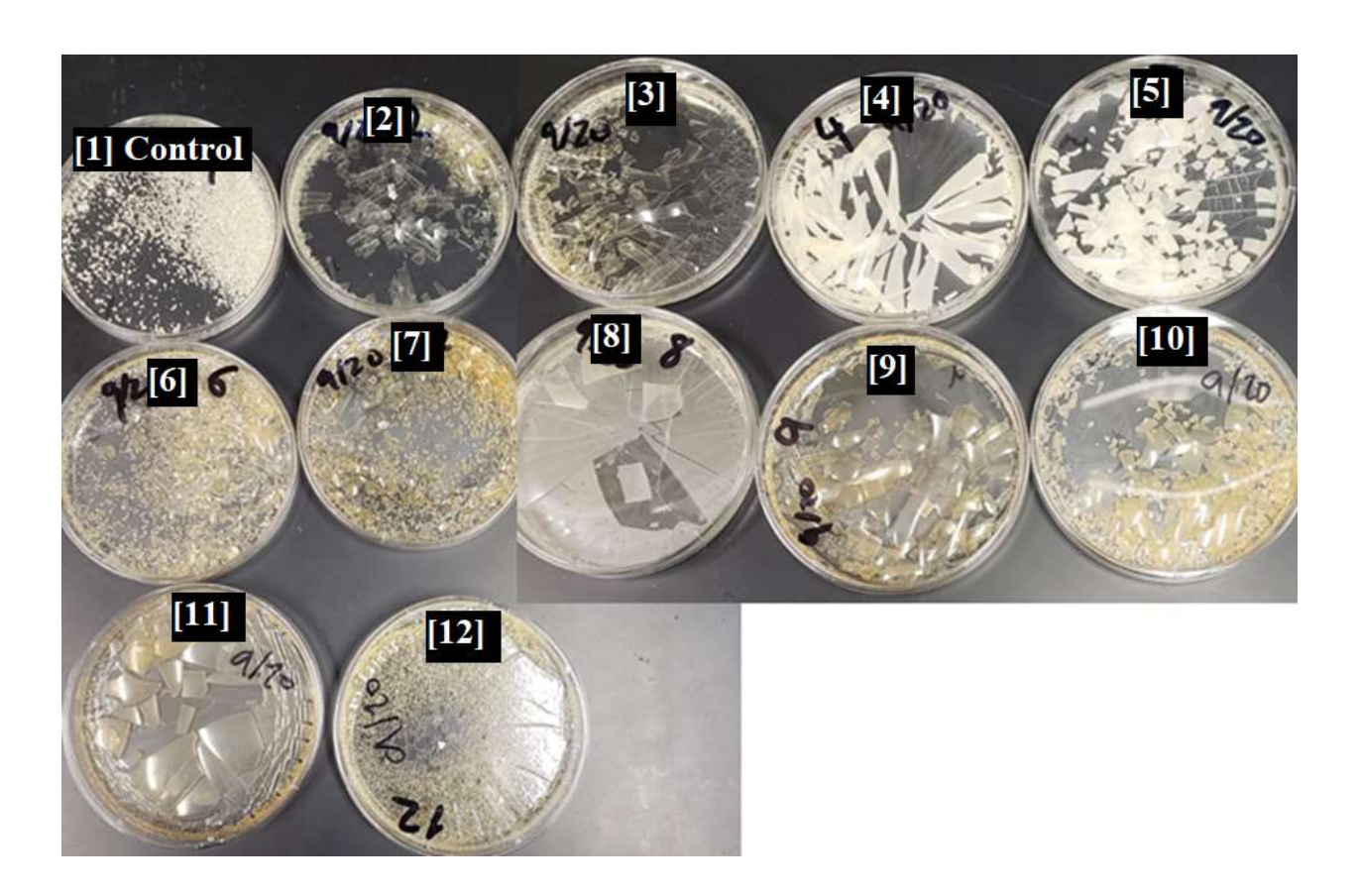


Figure 19: Preliminary experiment results (2 of 5) for whey protein isolate (WPI) and xylan standalone films crosslinked with transglutaminase (TG)

Note: Exact component ratios for treatments 1-12 are detailed in Table 14.

Trial 3

Film Formation:

Film preparation was performed according to the methods outlined in first trial. The plasticizer amounts were increased to achieve a 1:1 ratio. Both glycerol and sorbitol were used. TG and xylan were added to select films both separately and together. The relative amounts used in each treatment are detailed in Table 15 below. After 24 hours of drying, the films were qualitatively analyzed (Figure 20).

Observations:

While the films were no longer cracked, they were tacky and not able to be removed from the petri dishes into which they were cast. The glycerol films were gummier than those cast with sorbitol, so experiments proceeded with sorbitol exclusively in the next trial. A non-stick coated casting surface was tried as well.

Table 15: Preliminary experiment (3 of 5) treatment formulations for whey protein isolate (WPI) and xylan composite films crosslinked with transglutaminase (TG)

Note: Gly = glycerol; Sor = sorbitol

Film#	20% WPI Stock solution (mL)	WPI : plasticizer (ratio)	TG (IU)	WPI : xylan (ratio)	Phosphate Buffer (mL)
1	10	1.1:1 Sor			10
2	10	1.1:1 Sor	30		10
3	10	1.1:1 Sor		5:1	10
4	10	1.1:1 Sor	30	5:1	10
5	10	1.1:1 Gly			10
6	10	1.1:1 Gly	30		10
7	10	1.1:1 Gly		5:1	10
8	10	1.1:1 Gly	30	5:1	10



Figure 20: Preliminary experiment results (3 of 5) for whey protein isolate (WPI) and xylan standalone films crosslinked with transglutaminase (TG)

Note: Exact component ratios for treatments 1-8 are detailed in Table 15

Trial 4

Preparation:

Film preparation was performed according to the methods outlined in first trial. Films were cast onto a TeflonTM muffin tray to prevent adherence to the mold. More dilute WPI casting solutions were used to ensure complete drying. Glycerol was eliminated for use as a plasticizer. Xylan was added in increased ratios for a more complete trial. The relative amounts used in each treatment are detailed in Table 16 below. After 24 hours of drying, the films were qualitatively analyzed (Figure 21).

Observations:

Switching the mold to a Teflon[™] pan was an effective measure to produce films that were not cracked. The high plasticizer amount had a positive effect on reducing film brittleness. Films made without TG broke up in the casting try (Films 5-7), suggesting TG is required for film quality improvement. Diluting the WPI starting solution did not have an apparent effect on film quality. The films containing all three additives - sorbitol, TG, and xylan - were the most pliable, but also felt slightly tacky.

Table 16: Preliminary experiment (4 of 5) treatment formulations for whey protein isolate (WPI) and xylan composite films crosslinked with transglutaminase (TG)

Film#	10% WPI Stock solution (mL)	WPI : sorbitol (ratio)	TG (IU)	WPI : xylan (ratio)	Phosphate Buffer (mL)
1	10	1.5:1			1
2	8	1.2:1	30		3
3	8.5	1.3:1	30		2.5
4	9.5	1.5:1	30		2
5	8	1.2:1		4:1	4
6	8.5	1.3:1		5.7:1	3
7	9.5	1.5:1		9:1	2
8	8	1.2:1	30	4:1	4
9	8.5	1.3:1	30	5.7:1	3
10	9.5	1.5:1	30	9:1	2

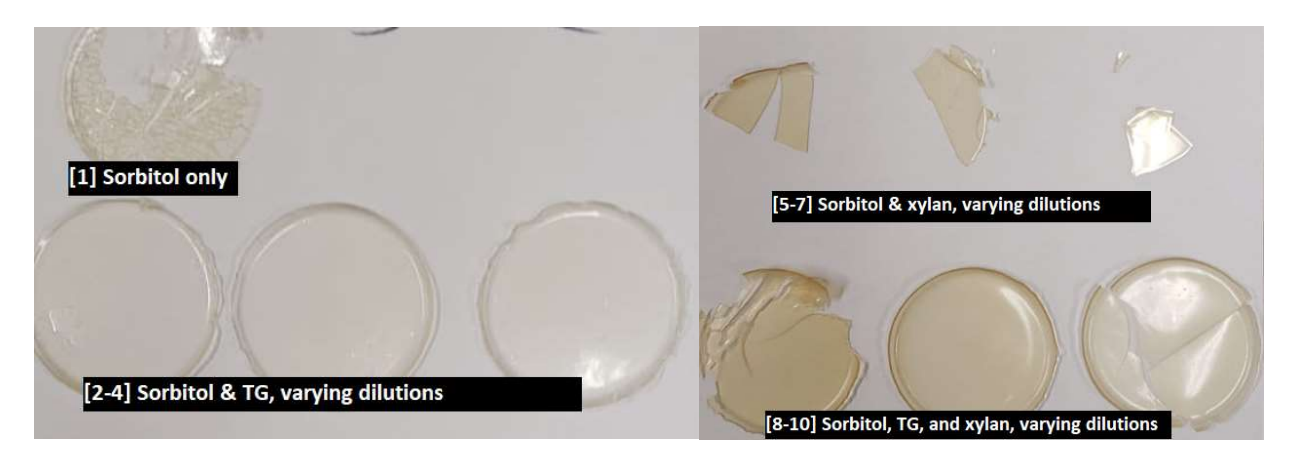


Figure 21: Preliminary experiment results (4 of 5) for whey protein isolate (WPI) and xylan standalone films crosslinked with transglutaminase (TG)

Note: Exact component ratios for treatments 1-10 are detailed in Table 16

Trial 5

Preparation:

A new film preparation strategy was utilized in the fifth trial, with different FFS preparation temperatures and conditions. A 5% w/w solution of WPI and sorbitol was prepared using only distilled water. Once these components were dissolved, the pH of was adjusted to 8.0 using 2N NaOH. This mixture was then heated to 90°C for 15 minutes. While still warm, the solution was homogenized for 2 minutes, then poured through a double layer of cheesecloth to remove resulting foam. The solution was left to equilibrate to room temperature over an hour. This was then used as a stock solution to which xylan and TG were added at room temperature. A control was made containing no TG. Each of the resulting films contained TG with increasing relative amounts of xylan. The relative amounts used in each treatment are detailed in Table 17 below. After 24 hours of drying, the films were qualitatively analyzed (Figure 22; Figure 21). Observations:

This film preparation method produced excellent standalone films. They were flexible, durable, and visually homogeneous. This preparation method was the most effective and was chosen as the strategy for this research. The sorbitol provided a good initial plasticizer, however after a week of conditioning, white patches began to appear on the film, thought to be crystallization (Figure 23). Glycerol was used to replace the sorbitol in the research FFS as the final change.

Table 17: Preliminary experiment (5 of 5) treatment formulations for whey protein isolate (WPI) and xylan composite films crosslinked with transglutaminase (TG)

Film#	5% w/w WPI Stock solution (mL)	WPI : sorbitol : xylan (ratio)	TG (IU)	Deionized water (mL)
1	8	1:1:0		2.5
2	8	1:1:0	30	2.5
3	8	10:10:1	30	2.5
4	8	5:5:1	30	2.5
5	8	3.3:3.3:1	30	2.5

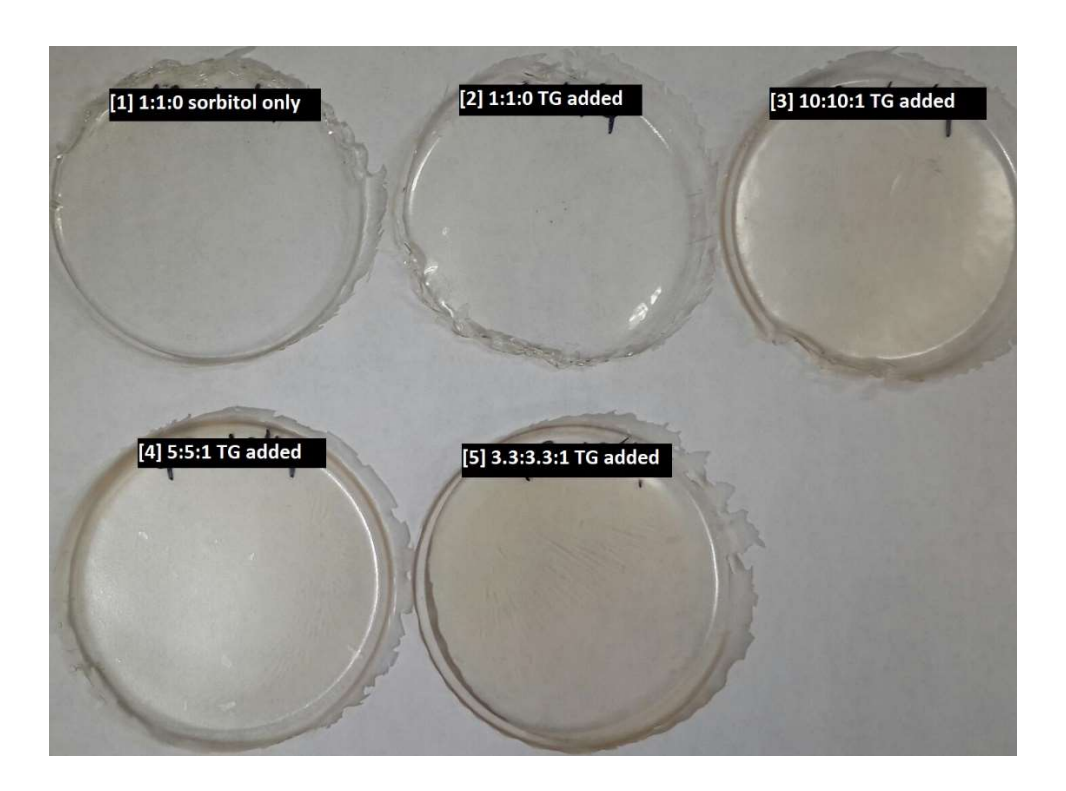


Figure 22: Preliminary experiment results (5 of 5) for whey protein isolate (WPI) and xylan standalone films crosslinked with transglutaminase (TG)

Note: Exact component ratios for treatments 1-5 are detailed in Table 17



 $\label{thm:condition} \textbf{Figure 23: Crystallization of the plasticizer sorbitol in whey protein isolate films after conditioning for 7 days$

REFERENCES

REFERENCES

- Akcan, T., Estévez, M., & Serdaroğlu, M. (2017). Antioxidant protection of cooked meatballs during frozen storage by whey protein edible films with phytochemicals from Laurus nobilis L. and Salvia officinalis. *LWT*, 77, 323–331. https://doi.org/10.1016/j.lwt.2016.11.051
- Albuquerque, T. L. de, da Silva, I. J., de Macedo, G. R., & Rocha, M. V. P. (2014). Biotechnological production of xylitol from lignocellulosic wastes: A review. *Process Biochemistry*, 49(11), 1779–1789. https://doi.org/10.1016/j.procbio.2014.07.010
- ASTM. (2013). F1249-13 Standard Test Method for Water Vapor Transmission Rate Through Plastic Film and Sheeting Using a Modulated Infrared Sensor. Retrieved from https://doi-org.proxy1.cl.msu.edu/10.1520/F1249-13
- ASTM. (2017). D3985-17 Standard Test Method for Oxygen Gas Transmission Rate Through Plastic Film and Sheeting Using a Coulometric Sensor. Retrieved from https://doi-org.proxy1.cl.msu.edu/10.1520/D3985-17
- ASTM. (2018). D882-18 Standard Test Method for Tensile Properties of Thin Plastic Sheeting. Retrieved from https://doi-org.proxy1.cl.msu.edu/10.1520/D0882-18
- Aziz, S. G.-G., & Almasi, H. (2018). Physical Characteristics, Release Properties, and Antioxidant and Antimicrobial Activities of Whey Protein Isolate Films Incorporated with Thyme (Thymus vulgaris L.) Extract-Loaded Nanoliposomes. *Food and Bioprocess Technology*, 11(8), 1552–1565. https://doi.org/10.1007/s11947-018-2121-6
- Bahram, S., Rezaei, M., Soltani, M., Kamali, A., Ojagh, S. M., & Abdollahi, M. (2014). Whey Protein Concentrate Edible Film Activated with Cinnamon Essential Oil. *Journal of Food Processing and Preservation*, 38(3), 1251–1258. https://doi.org/10.1111/jfpp.12086
- Beg, Q., Kapoor, M., Mahajan, L., & Hoondal, G. (2001). Microbial xylanases and their industrial applications: a review. *Applied Microbiology and Biotechnology*, *56*(3), 326–338. https://doi.org/10.1007/s002530100704
- Brandt, A., Gräsvik, J., Hallett, J. P., & Welton, T. (2013). Deconstruction of lignocellulosic biomass with ionic liquids. *Green Chemistry*, *15*(3), 550–583. https://doi.org/10.1039/C2GC36364J
- Carà, P. D., Pagliaro, M., Elmekawy, A., Brown, David. R., Verschuren, P., Shiju, N. R., & Rothenberg, G. (2013). Hemicellulose hydrolysis catalysed by solid acids. *Catalysis Science & Technology*, 3(8), 2057. https://doi.org/10.1039/c3cy20838a

- Chakravartula, S. S. N., Soccio, M., Lotti, N., Balestra, F., Dalla Rosa, M., & Siracusa, V. (2019). Characterization of Composite Edible Films Based on Pectin/Alginate/Whey Protein Concentrate. *Materials*, 12(15), 2454. https://doi.org/10.3390/ma12152454
- Chambi, H., & Grosso, C. (2006). Edible films produced with gelatin and casein cross-linked with transglutaminase. *Food Research International*, *39*(4), 458–466. https://doi.org/10.1016/j.foodres.2005.09.009
- Cheng, L. H., Abd Karim, A., & Seow, C. C. (2008). Characterisation of composite films made of konjac glucomannan (KGM), carboxymethyl cellulose (CMC) and lipid. *Food Chemistry*, 107(1), 411–418. https://doi.org/10.1016/j.foodchem.2007.08.068
- Chevalier, E., Chaabani, A., Assezat, G., Prochazka, F., & Oulahal, N. (2018). Casein/wax blend extrusion for production of edible films as carriers of potassium sorbate—A comparative study of waxes and potassium sorbate effect. *Food Packaging and Shelf Life*, *16*, 41–50. https://doi.org/10.1016/j.fpsl.2018.01.005
- CRC. (2019). CRC Handbook of Chemistry and Physics (100th ed.). CRC Press. http://hbcponline.com.proxy2.cl.msu.edu/faces/contents/ContentsSearch.xhtml;jsessionid =FE87593B4C99A76A4F591BA5408F5157
- Di Pierro, P., Chico, B., Villalonga, R., Mariniello, L., Damiao, A. E., Masi, P., & Porta, R. (2006). Chitosan—Whey Protein Edible Films Produced in the Absence or Presence of Transglutaminase: Analysis of Their Mechanical and Barrier Properties.

 Biomacromolecules, 7(3), 744–749. https://doi.org/10.1021/bm050661u
- Ebringerová, A., & Heinze, T. (2000). Xylan and xylan derivatives biopolymers with valuable properties, 1. Naturally occurring xylans structures, isolation procedures and properties. *Macromolecular Rapid Communications*, 21(9), 542–556. https://doi.org/10.1002/1521-3927(20000601)21:9<542::AID-MARC542>3.0.CO;2-7
- Edwards, P. J. B., & Jameson, G. B. (2014). Structure and Stability of Whey Proteins. In *Milk Proteins: From Expression to Food* (2nd ed., pp. 201–242). Academic Press.
- Farrell, H. M., Jimenez-Flores, R., Bleck, G. T., Brown, E. M., Butler, J. E., Creamer, L. K., Hicks, C. L., Hollar, C. M., Ng-Kwai-Hang, K. F., & Swaisgood, H. E. (2004). Nomenclature of the Proteins of Cows' Milk—Sixth Revision. *Journal of Dairy Science*, 87(6), 1641–1674. https://doi.org/10.3168/jds.S0022-0302(04)73319-6
- Galbe, M., & Zacchi, G. (2002). A review of the production of ethanol from softwood. *Applied Microbiology and Biotechnology*, 59(6), 618–628. Scopus. https://doi.org/10.1007/s00253-002-1058-9
- Galus, S., & Kadzińska, J. (2015). Food applications of emulsion-based edible films and coatings. *Trends in Food Science & Technology*, 45(2), 273–283. https://doi.org/10.1016/j.tifs.2015.07.011

- Galus, S., & Kadzińska, J. (2016). Whey protein edible films modified with almond and walnut oils. *Food Hydrocolloids*, *52*, 78–86. https://doi.org/10.1016/j.foodhyd.2015.06.013
- Goksu, E. I., Karamanlioglu, M., Bakir, U., Yilmaz, L., & Yilmazer, U. (2007). Production and Characterization of Films from Cotton Stalk Xylan. *Journal of Agricultural and Food Chemistry*, 55(26), 10685–10691. https://doi.org/10.1021/jf071893i
- Gounga, M. E., Xu, S.-Y., & Wang, Z. (2010). Film Forming Mechanism and Mechanical and Thermal Properties of Whey Protein Isolate-Based Edible Films as Affected by Protein Concentration, Glycerol Ratio and Pullulan Content. *Journal of Food Biochemistry*, 34(3), 501–519. https://doi.org/10.1111/j.1745-4514.2009.00294.x
- Griko, Y. V., & Remeta, D. P. (1999). Energetics of solvent and ligand-induced conformational changes in α-lactalbumin. *Protein Science*, 8(3), 554–561. https://doi.org/10.1110/ps.8.3.554
- Gurdian, C., Chouljenko, A., Solval, K. M., Boeneke, C., King, J. M., & Sathivel, S. (2017). Application of Edible Films Containing Oregano (Origanum vulgare) Essential Oil on Queso Blanco Cheese Prepared with Flaxseed (Linum usitatissimum) Oil. *Journal of Food Science*, 82(6), 1395–1401. https://doi.org/10.1111/1750-3841.13733
- Hahn-Hägerdal, B., Wahlbom, C. F., Gárdonyi, M., van Zyl, W. H., Otero, R. R. C., & Jönsson, L. J. (2001). Metabolic Engineering of Saccharomyces cerevisiae for Xylose Utilization. In J. Nielsen, L. Eggeling, J. Dynesen, M. Gárdonyi, R. T. Gill, A. A. de Graaf, B. Hahn-Hägerdal, L. J. Jönsson, C. Khosla, R. Licari, R. McDaniel, M. McIntyre, C. Miiller, J. Nielsen, R. R. Cordero Otero, H. Sahm, U. Sauer, D. E. Stafford, G. Stephanopoulos, ... W. H. van Zyl (Eds.), Metabolic Engineering (Vol. 73, pp. 53–84). Springer Berlin Heidelberg. https://doi.org/10.1007/3-540-45300-8_4
- Hassan, B., Chatha, S. A. S., Hussain, A. I., Zia, K. M., & Akhtar, N. (2018). Recent advances on polysaccharides, lipids and protein based edible films and coatings: A review. *International Journal of Biological Macromolecules*, 109, 1095–1107. https://doi.org/10.1016/j.ijbiomac.2017.11.097
- Heine, W. E., Klein, P. D., & Reeds, P. J. (1991). The Importance of α-Lactalbumin in Infant Nutrition. *The Journal of Nutrition*, 121(3), 277–283. https://doi.org/10.1093/jn/121.3.277
- Holm, N. K., Jespersen, S. K., Thomassen, L. V., Wolff, T. Y., Sehgal, P., Thomsen, L. A., Christiansen, G., Andersen, C. B., Knudsen, A. D., & Otzen, D. E. (2007). Aggregation and fibrillation of bovine serum albumin. *Biochimica et Biophysica Acta (BBA) Proteins and Proteomics*, 1774(9), 1128–1138. https://doi.org/10.1016/j.bbapap.2007.06.008

- Hong, S.-I., & Krochta, J. M. (2006). Oxygen barrier performance of whey-protein-coated plastic films as affected by temperature, relative humidity, base film and protein type. *Journal of Food Engineering*, 77(3), 739–745. https://doi.org/10.1016/j.jfoodeng.2005.07.034
- Janjarasskul, T., Rauch, D. J., McCarthy, K. L., & Krochta, J. M. (2014). Barrier and tensile properties of whey protein—candelilla wax film/sheet. *LWT Food Science and Technology*, *56*(2), 377–382. https://doi.org/10.1016/j.lwt.2013.11.034
- Jiang, S., Zhang, T., Song, Y., Qian, F., Tuo, Y., & Mu, G. (2019). Mechanical properties of whey protein concentrate based film improved by the coexistence of nanocrystalline cellulose and transglutaminase. *International Journal of Biological Macromolecules*, 126, 1266–1272. https://doi.org/10.1016/j.ijbiomac.2018.12.254
- Jiang, S., Zhang, X., Ma, Y., Tuo, Y., Qian, F., Fu, W., & Mu, G. (2016). Characterization of whey protein-carboxymethylated chitosan composite films with and without transglutaminase treatment. *Carbohydrate Polymers*, 153, 153–159. https://doi.org/10.1016/j.carbpol.2016.07.094
- Jiang, Z., Wang, C., Li, T., Sun, D., Gao, H., Gao, Z., & Mu, Z. (2019). Effect of ultrasound on the structure and functional properties of transglutaminase-crosslinked whey protein isolate exposed to prior heat treatment. *International Dairy Journal*, 88, 79–88. https://doi.org/10.1016/j.idairyj.2018.08.007
- Jost, V., & Stramm, C. (2016). Influence of plasticizers on the mechanical and barrier properties of cast biopolymer films. *Journal of Applied Polymer Science*, 133(2). https://doi.org/10.1002/app.42513
- Kadam, D. M., Thunga, M., Wang, S., Kessler, M. R., Grewell, D., Lamsal, B., & Yu, C. (2013). Preparation and characterization of whey protein isolate films reinforced with porous silica coated titania nanoparticles. *Journal of Food Engineering*, 117(1), 133–140. https://doi.org/10.1016/j.jfoodeng.2013.01.046
- Kayserilioğlu, B. Ş., Bakir, U., Yilmaz, L., & Akkaş, N. (2003). Use of xylan, an agricultural by-product, in wheat gluten based biodegradable films: mechanical, solubility and water vapor transfer rate properties. *Bioresource Technology*, 87(3), 239–246. https://doi.org/10.1016/S0960-8524(02)00258-4
- Kieliszek, M., & Misiewicz, A. (2014). Microbial transglutaminase and its application in the food industry. A review. *Folia Microbiologica*, *59*(3), 241–250. https://doi.org/10.1007/s12223-013-0287-x
- Krogars, K., Heinämäki, J., Karjalainen, M., Niskanen, A., Leskelä, M., & Yliruusi, J. (2003). Enhanced stability of rubbery amylose-rich maize starch films plasticized with a combination of sorbitol and glycerol. *International Journal of Pharmaceutics*, *251*(1), 205–208. https://doi.org/10.1016/S0378-5173(02)00585-9

- Lin, H.-C., Wang, B.-J., & Weng, Y.-M. (2020). Development and characterization of sodium caseinate edible films cross-linked with genipin. *LWT*, *118*, 108813. https://doi.org/10.1016/j.lwt.2019.108813
- McHugh, T. H., & Krochta, J. M. (1994). Sorbitol- vs Glycerol-Plasticized Whey Protein Edible Films: Integrated Oxygen Permeability and Tensile Property Evaluation. *Journal of Agricultural and Food Chemistry*, 42(4), 841–845. https://doi.org/10.1021/jf00040a001
- Mehdizadeh, T., Tajik, H., Razavi Rohani, S. M., & Oromiehie, A. R. (2012). Antibacterial, antioxidant and optical properties of edible starch-chitosan composite film containing Thymus kotschyanus essential oil. *Veterinary Research Forum*, *3*(3), 167–173.
- Militello, V., Vetri, V., & Leone, M. (2003). Conformational changes involved in thermal aggregation processes of bovine serum albumin. *Biophysical Chemistry*, *105*(1), 133–141. https://doi.org/10.1016/S0301-4622(03)00153-4
- Morr, C. V., & Ha, E. Y. W. (1993). Whey protein concentrates and isolates: Processing and functional properties. *Critical Reviews in Food Science and Nutrition*, *33*(6), 431–476. https://doi.org/10.1080/10408399309527643
- Naidu, D. S., Hlangothi, S. P., & John, M. J. (2018). Bio-based products from xylan: A review. *Carbohydrate Polymers*, 179, 28–41. https://doi.org/10.1016/j.carbpol.2017.09.064
- Nicolai, T., Britten, M., & Schmitt, C. (2011). β-Lactoglobulin and WPI aggregates: Formation, structure and applications. *Food Hydrocolloids*, *25*(8), 1945–1962. https://doi.org/10.1016/j.foodhyd.2011.02.006
- O'Brien, D. (2018). That's a Wrap: Edible Food Wraps from ARS. *Agricultural Research*, 66(2). https://agresearchmag.ars.usda.gov/2018/feb/wraps/
- Olson, A. C., Gray, G. M., Chiu, M.-C., & Fleming, S. E. (1983). Cellulose, Xylan, Corn Bran, and Pectin in the Human Digestive Process. In I. Furda (Ed.), *Unconventional Sources of Dietary Fiber* (Vol. 214, pp. 221–239). AMERICAN CHEMICAL SOCIETY. https://doi.org/10.1021/bk-1983-0214.ch016
- Peña, I., Mata, S., Martín, A., Cabezas, C., Daly, A. M., & Alonso, J. L. (2013). Conformations of D-xylose: the pivotal role of the intramolecular hydrogen-bonding. *Physical Chemistry Chemical Physics*, 15(41), 18243–18248. https://doi.org/10.1039/C3CP52345D
- Porta, R., Mariniello, L., Pierro, P. D., Sorrentino, A., & Giosafatto, C. V. L. (2011). Transglutaminase Crosslinked Pectin- and Chitosan-based Edible Films: A Review. *Critical Reviews in Food Science and Nutrition*, *51*(3), 223–238. https://doi.org/10.1080/10408390903548891

- Prommakool, A., Sajjaanantakul, T., Janjarasskul, T., & Krochta, J. M. (2011). Whey proteinokra polysaccharide fraction blend edible films: tensile properties, water vapor permeability and oxygen permeability. *Journal of the Science of Food and Agriculture*, 91(2), 362–369. https://doi.org/10.1002/jsfa.4194
- Qazanfarzadeh, Z., & Kadivar, M. (2016). Properties of whey protein isolate nanocomposite films reinforced with nanocellulose isolated from oat husk. *International Journal of Biological Macromolecules*, *91*, 1134–1140. https://doi.org/10.1016/j.ijbiomac.2016.06.077
- Quan, W., Zhang, C., Zheng, M., Lu, Z., & Lu, F. (2018). Whey protein isolate with improved film properties through cross-linking catalyzed by small laccase from Streptomyces coelicolor. *Journal of the Science of Food and Agriculture*, 98(10), 3843–3850. https://doi.org/10.1002/jsfa.8900
- Ramos, Ó. L., Fernandes, J. C., Silva, S. I., Pintado, M. E., & Malcata, F. X. (2012). Edible Films and Coatings from Whey Proteins: A Review on Formulation, and on Mechanical and Bioactive Properties. *Critical Reviews in Food Science and Nutrition*, *52*(6), 533–552. https://doi.org/10.1080/10408398.2010.500528
- Ramos, Ó. L., Reinas, I., Silva, S. I., Fernandes, J. C., Cerqueira, M. A., Pereira, R. N., Vicente, A. A., Poças, M. F., Pintado, M. E., & Malcata, F. X. (2013). Effect of whey protein purity and glycerol content upon physical properties of edible films manufactured therefrom. *Food Hydrocolloids*, 30(1), 110–122. https://doi.org/10.1016/j.foodhyd.2012.05.001
- Sabiha-Hanim, S., & Siti-Norsafurah, A. M. (2012). Physical Properties of Hemicellulose Films from Sugarcane Bagasse. *Procedia Engineering*, *42*, 1390–1395. https://doi.org/10.1016/j.proeng.2012.07.532
- Scheller, H. V., & Ulvskov, P. (2010). Hemicelluloses. *Annual Review of Plant Biology*, 61(1), 263–289. https://doi.org/10.1146/annurev-arplant-042809-112315
- Schmid, M., Sängerlaub, S., Wege, L., & Stäbler, A. (2014). Properties of Transglutaminase Crosslinked Whey Protein Isolate Coatings and Cast Films. *Packaging Technology and Science*, *27*(10), 799–817. https://doi.org/10.1002/pts.2071
- Selke, S. E. M., & Culter, J. D. (2016). 3 Polymer Structure and Properties. In S. E. M. Selke & J. D. Culter (Eds.), *Plastics Packaging (Third Edition)* (pp. 23–100). Hanser. https://doi.org/10.3139/9783446437197.003
- Shokri, S., Ehsani, A., & Jasour, M. S. (2015). Efficacy of Lactoperoxidase System-Whey Protein Coating on Shelf-life Extension of Rainbow Trout Fillets During Cold Storage(4 °C). *Food and Bioprocess Technology*, 8(1), 54–62. https://doi.org/10.1007/s11947-014-1378-7

- Skulcova, A., Majova, V., Kohutova, M., Grosik, M., Sima, J., & Jablonsky, M. (2017). UV/Vis Spectrometry as a Quantification Tool for Lignin Solubilized in Deep Eutectic Solvents. *BioResources*, *12*(3), 6713–6722.
- Sukyai, P., Anongjanya, P., Bunyahwuthakul, N., Kongsin, K., Harnkarnsujarit, N., Sukatta, U., Sothornvit, R., & Chollakup, R. (2018). Effect of cellulose nanocrystals from sugarcane bagasse on whey protein isolate-based films. *Food Research International*, 107, 528–535. https://doi.org/10.1016/j.foodres.2018.02.052
- Trezza, T. A., & Krochta, J. M. (2000). Color Stability of Edible Coatings During Prolonged Storage. *Journal of Food Science*, 65(7), 1166–1169. https://doi.org/10.1111/j.1365-2621.2000.tb10259.x
- US EPA, (2017). Containers and Packaging: Product-Specific Data. US EPA. https://www.epa.gov/facts-and-figures-about-materials-waste-and-recycling/containers-and-packaging-product-specific-data
- Yadav, J. S. S., Yan, S., Pilli, S., Kumar, L., Tyagi, R. D., & Surampalli, R. Y. (2015). Cheese whey: A potential resource to transform into bioprotein, functional/nutritional proteins and bioactive peptides. *Biotechnology Advances*, 33(6, Part 1), 756–774. https://doi.org/10.1016/j.biotechadv.2015.07.002
- Yoo, S., & Krochta, J. M. (2011). Whey protein–polysaccharide blended edible film formation and barrier, tensile, thermal and transparency properties. *Journal of the Science of Food and Agriculture*, *91*(14), 2628–2636. https://doi.org/10.1002/jsfa.4502
- Zhang, P., & Whistler, R. L. (2004). Mechanical properties and water vapor permeability of thin film from corn hull arabinoxylan. *Journal of Applied Polymer Science*, 93(6), 2896–2902. https://doi.org/10.1002/app.20910